The Role of Mountains in the South Asian Monsoon Circulation

DOUGLAS G. HAHN AND SYUKURO MANABE

Geophysical Fluid Dynamics Laboratory/NOAA, Princeton University, Princeton, N. J. 08540

(Manuscript received 29 October 1974, in revised form 12 May 1975)

ABSTRACT

An 11-level numerical model of the atmospheric circulation which has a prescribed seasonal variation of insolation and sea surface temperatures is integrated with respect to time for approximately three model years. The model is global in domain and incorporates a smoothed mountain topography. In order to investigate the role that mountains play in the south Asian monsoon circulation, a second numerical experiment, exactly the same as the first except that all mountains are removed, is integrated with respect to time from 25 March through July.

Analysis of the model with mountains reveals that the large-scale circulation associated with the south Asian monsoon is well simulated. However, the onset of the monsoon is approximately 10–15 days later than normal, and the atmosphere over the western Pacific seems to be dynamically too active, while the atmosphere over the northern reaches of the Bay of Bengal and northern India is relatively inactive.

Comparison of the simulation with mountains with the simulation without mountains reveals that the presence of mountains is instrumental in maintaining the south Asian low pressure system as the continental low forms far to the north and east in the simulation without mountain topography. In the model with mountains, much higher temperatures are maintained in the middle and upper troposphere over the Tibetan Plateau, a region where upward motion and latent heating dominate. Without mountains, downward motion and sensible heating by the earth's surface dominate in this region. In the simulation with mountains, high temperatures over Tibet produce a low pressure envelope over these mountains which extends southward over the plains of south Asia. The low pressure belt being located farther south than in the simulation without mountains produces a stronger north-south pressure gradient which enables moist southerly flow at the surface to penetrate farther northward into Asia. Many of the features of the monsoon break persist in the model without mountains as copious precipitation extends northward only to south India. Clearly, mountain effects help to extend a monsoon climate farther north onto the Asian continent.

The evolution of the south Asian monsoon is also influenced by the effects of mountains. Near the time of onset in the model with mountains, the subtropical jet abruptly jumps northward from a latitude just south of Tibet, 25°N, to a mean summertime position along 45°N. In the model without mountains, the subtropical jet gradually moves northward over a period of about two months, finally reaching a summertime position approximately 10° farther south than in the model with mountains. At the time of onset in the model with mountains, humid southerly flow near the earth's surface suddenly extends northward from equatorial latitudes to the south Asian low pressure belt centered at 30°N. In the model without mountains, humid southerly flow extends northward from equatorial regions, but it doesn't extend as far northward as northern and central India. These differences are attributed to mechanical and thermodynamical effects of the Tibetan Plateau.

1. Introduction

In the classical literature, the large-scale flow patterns associated with the south Asian summer monsoon were described to result principally from the interaction of the annual cycle of solar radiation and the differential effective heat capacities of land and ocean water. Halley, in 1686, described the Asian monsoon circulation as resembling a giant sea breeze resulting from land-sea contrasts. His description qualitatively explains the large-scale monsoon circulation features: the southeasterly trades near the surface in the Southern Hemisphere crossing the equator and approaching the continental heat low as a southwesterly flow, vertical motion over the relatively hot continent transporting sensible and released latent heat upward into the upper troposphere, and the seasonal, upper-tropospheric northeasterly jet transporting air back into the Southern Hemisphere. However, recent observational investigations make us aware that Halley's description is far from complete (Walker, 1972).

One of the most difficult factors to assess is the role that mountains play in the large-scale south Asian monsoon. A hypothesis first presented by Flohn (1950, 1953, 1960), that the Tibetan Plateau acts as an elevated sensible heat source during the summer season, generating a warm core anticyclone in the upper troposphere, was thought by some to be the primary mechanism for establishing the monsoon circulation over south Asia. Riehl (1959) indicated that latent heating, rather than sensible heating, may be the

primary mechanism for maintaining the south Asian monsoon. Later, Flohn (1968), having data from the Chinese People's Republic at his disposal, presented results from his observational study which concluded that the effect of sensible heating by the Tibetan Plateau is important in the western arid regions and that the effect of latent heat released orographically over the southeastern corner of Tibet, before as well as after onset of the monsoon, is particularly instrumental in developing and maintaining a thermal anticyclone over the Himalayas. Flohn described the Tibet Highlands as "a heat engine with a giant chimney in their southeastern corner."

Rangarajan and others are skeptical of Flohn's ideas. Rangarajan (1963) points out that snow fields cover the high elevations of Tibet in summer making the elevated plateau an unlikely candidate for sensible heating of the middle troposphere. He analyzed monthly mean 500 mb temperature fields over south Asia [later found to have possible systematic errors (Flohn, 1968)] and concluded that mountains are not directly responsible for the high mid-tropospheric temperatures in this region. Rangarajan then re-emphasized a more classical theory, similar to Halley's (1686), for explaining the south Asian monsoon circulation.

Aside from the controversy over how the thermal effects of the Tibetan Plateau influence the development and maintenance of the south Asian monsoon, there also seem to be differing viewpoints regarding the influence that the mountains have on the abrupt shift of the subtropical jet which usually takes place just before the onset of the monsoon. According to Yin (1949), the onset of the monsoon begins with a northward shift of the subtropical jet in the upper troposphere over Tibet. The current ceases to flow to the south of the Tibetan Highlands and quickly jumps to a northerly course along the northern fringes of the mountain range. This abrupt rearrangement is attributed, at least in part, to the mechanical influences of the Tibetan Plateau. Different viewpoints are held by Yeh *et al.* (1959) and Staff Members (1957) who analyzed 5-day mean cross sections of the observed zonal wind and found that similar jumps can be found in the upper air circulation at many longitudes away from the Asian region. According to Yeh *et al.* as the elevation of the sun increases from winter to summer in the Northern Hemisphere, the temperature contrast decreases from pole to equator until it reaches a threshold value when a certain type of instability in the atmosphere appears. This results in an abrupt change in the upper air circulation which is not directly related to mountain effects.

One effective method of identifying the role of mountains in the monsoon circulation is to perform numerical simulation experiments using mathematical models of the atmosphere. Numerical studies by Mintz and Arakawa (Mintz, 1965) and Manabe and Terpstra (1974) indicate that mountains play an important role in the circulation patterns over Asia during winter months. For the summer case, Murakami *et al.* (1970) did a study contrasting July circulation patterns with and without mountains using an 8-level two-dimensional hemispheric model of the Indian monsoon along 80°E. They were able to obtain realistic zonal wind simulations only when the effects of mountains were incorporated in their model. However, because of computational difficulties arising from the effect of mountains themselves, they did not discuss in detail the results of their experiment with mountains. Washington and Daggupaty (1975) were able to simulate some of the features of the monsoon circulation using a global model of the atmosphere. Their model, however, produces a belt of maximum rainfall just north of the equator over the mid-Indian Ocean. As of now, they have not attempted to identify the role of mountains in this experiment.

The discussions in the preceding paragraphs indicate that we do not know precisely how mountains affect the summer monsoon circulation. This study represents an attempt to answer this question using a global general circulation model developed at the Geophysical Fluid Dynamics Laboratory (GFDL). The performance of this model has been extensively documented by Manabe *et al.* (1974), Manabe and Holloway (1975), Krishnamurti *et al.* (1973), Hayashi (1974) and Shukla (1975). It has been demonstrated in these papers that the model successfully simulates some of the important features of the south Asian monsoon, such as the easterly jet and the seasonal reversal of the surface flow over the north Indian Ocean. Encouraged by their success, we decided to perform another numerical experiment using the general circulation model with all mountains removed. By comparing the results of the experiment with no mountains (hereafter referred to as the NM-model) with the results of the original experiment which includes mountain topography (hereafter referred to as the M-model), it is hoped that the role of mountains in the south Asian summer monsoon will be more clearly identified.

2. Brief description of the models

The M-model is identical to the global model which was constructed and described by Manabe *et al.* (1974). It is global in extent and undergoes seasonal (but not diurnal) variations of insolation and sea surface temperature. A comprehensive description of the major components of the M-model is contained in a paper by Holloway and Manabe (1971). Therefore, only a brief outline of the model is presented here and the reader is referred to the above-mentioned papers for a more detailed description.

The M-model incorporates the primitive equations formulated in the sigma coordinate system (Phillips, 1957). In the sigma system, the ground is a coordinate surface so that the effect of mountains can be easily incorporated without introducing problems associated with uncentered horizontal differencing. In the vertical,

11 unevenly spaced finite-difference levels are chosen so that the model can simulate the structure of the atmosphere from the planetary boundary layer up to a stratospheric level at approximately 31 km. In the horizontal, the global grid system of Kurihara and Holloway (1967) is modified such that a horizontal resolution of approximately 270 km is as uniform as possible (see Fig. 2.2 of Manabe *et al.*, 1974).

For simulation of the general circulation with mountains, surface height data were obtained from the Scripps Institution of Oceanography (Smith *et al.*, 1966). The surface height field is smoothed using a method described by Holloway and Manabe (1971) so that the scale of variation in land heights is not smaller than the horizontal grid scale. Obviously, use of smoothed topography has important effects on rainfall and surface flow patterns since it systematically lowers and broadens tall, narrow mountain ranges. This aspect will be discussed in later sections. Fig. 2.1 shows the smoothed surface height field for the south Asian monsoon region. The reader is referred to Manabe and Holloway (1975) for the global distribution of smoothed topography.

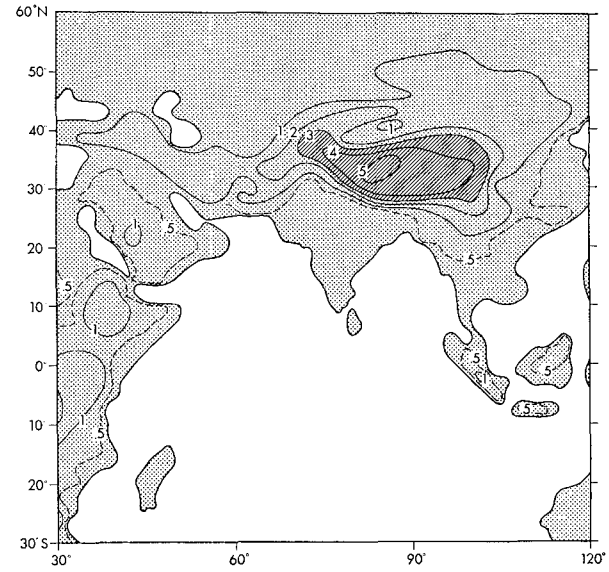

FIG. 2.1. Horizontal distribution of smoothed surface elevations (km) for the south Asian monsoon region of the general circulation model with mountains.

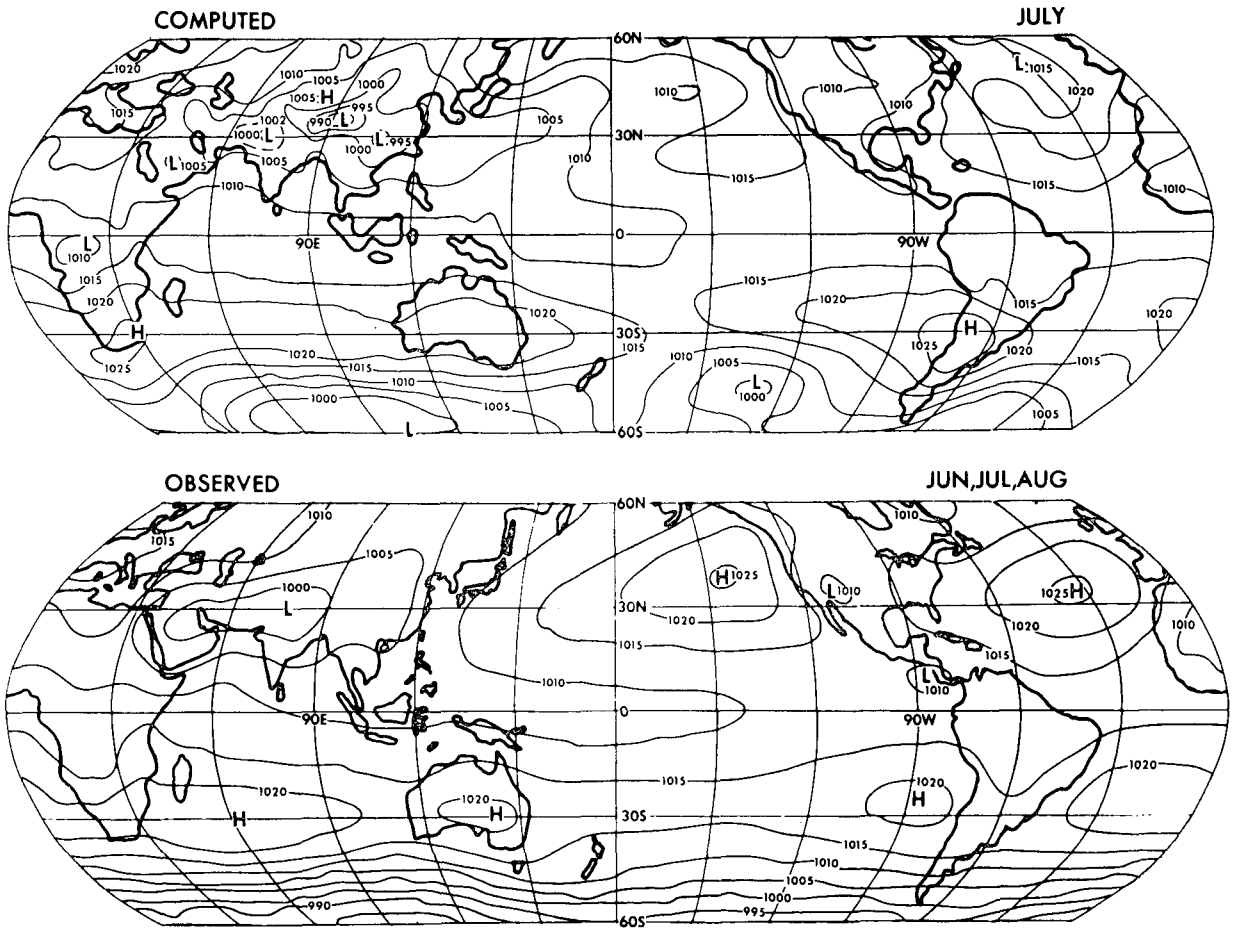

FIG. 3.1. Horizontal distributions of mean sea level pressure (mb). Top, computed July mean of the M-model; bottom, observed June-July-August mean (Newell *et al.*, 1972).

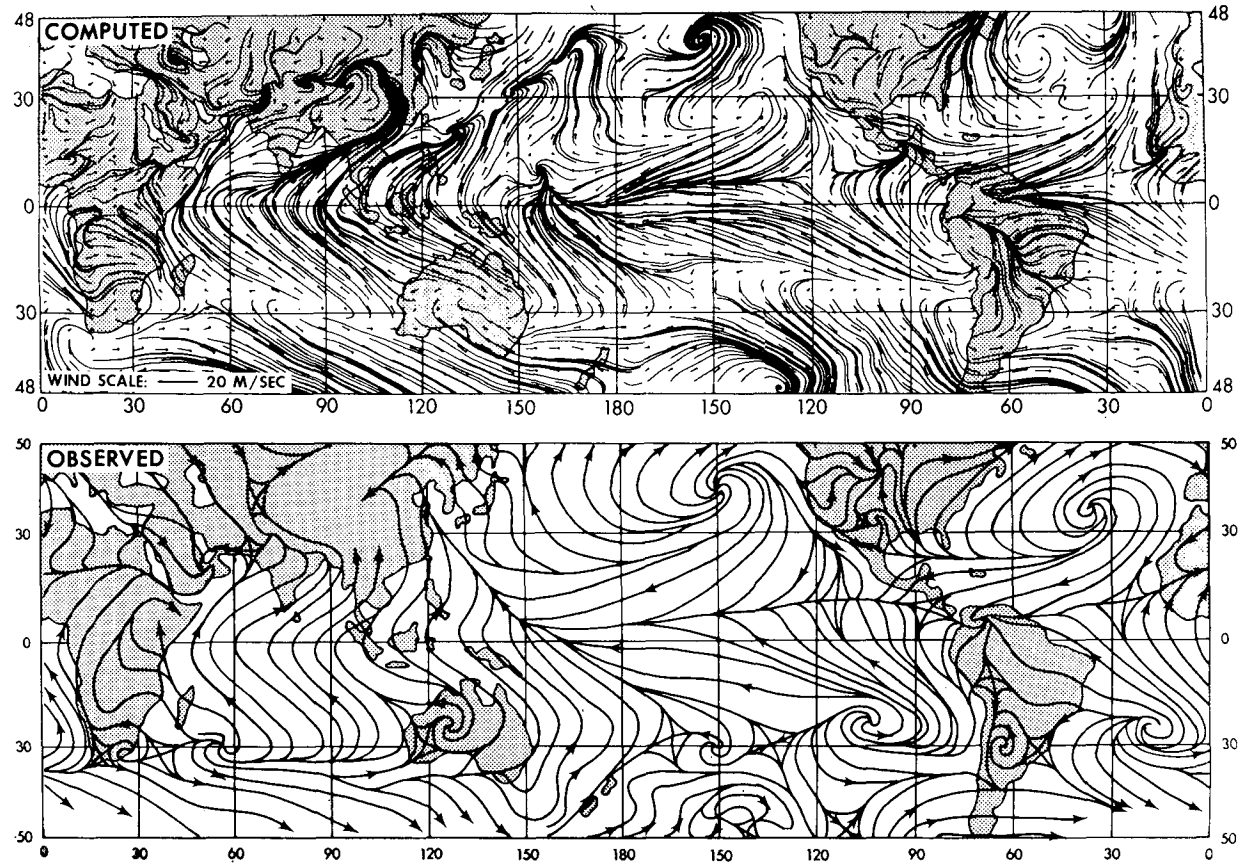

FIG. 3.2. Top, July mean vectors and streamlines near the earth's surface ($\sigma = P/P_* = 0.99$; P = pressure, P_* = surface pressure) of the M-model; bottom, observed July mean streamlines at the earth's surface (Mintz and Dean, 1952).

The numerical time integration of the M-model extended for 3.5 model years. For the first 1.5 model years, this model was time-integrated on a modified Kurihara-Holloway grid of approximately 540 km horizontal resolution. The final 2 model years were time-integrated on a high-resolution (270 km) grid. The monsoon circulation is successfully simulated in all model years; however, only data from the last year of simulation will be presented in this paper.

The first part of this paper is devoted to a detailed description of the M-model's simulation of the south Asian monsoon. The second part of this paper is devoted to a study of the effects of mountains on the south Asian monsoon by comparing results from the M-model with those from the NM-model. For the NM-model, the same identical computer code is used. The initial conditions are taken from a computer data tape of the M-model corresponding to 25 March of the final model year. All land elevations are eliminated. In order to reduce the magnitude of surface pressure adjustment responding to the large change in land elevations, surface pressures are initially set to 988 mb everywhere rather than using surface pressures from the M-model. The NM-model is time-integrated from 25 March through 31 July.

3. Monsoon as simulated with mountains

a. Sea level pressure

The July time-mean sea level pressure patterns as simulated by the M-model are shown in Fig. 3.1 [the method of computing sea level pressure is found in Holloway and Manabe (1971)]. Over most of the Eastern Hemisphere in July, when the monsoon circulation is well-developed, the sea level pressure field is characterized by a downward sloping pressure gradient from the subtropical anticyclones, centered at about 30°S, toward the south Asian low pressure belt centered at about 30°N. Fig. 3.1 shows that the large-scale pressure pattern is similar to the observed distribution (Newell *et al.*, 1972) for the June–August period. The computed south Asian low pressure belt extends from Arabia across Asia and into the western Pacific. The low pressure belt extending into the western Pacific is somewhat unrealistic and results from a large number of tropical cyclones which move along the coast

in this region. When tropical cyclones are prevalent, it is not uncommon, according to Sadler (private communication), to observe similar pressure distributions for short periods in July over the western Pacific. However, this low pressure feature does not regularly show up in observed monthly mean pressure distributions.

The lowest pressure of the south Asian low as simulated by the model is centered near the highest point of the Tibetan Plateau. It is too deep and located too far toward the east. Some of this discrepancy in the vicinity of the mountains may be explained by the large extrapolation of surface pressure to sea level over Tibet.

A more detailed look at the simulated pressure distribution reveals that another center of low pressure, commonly called the monsoon trough, is located in northwestern India (represented by the 1002 mb dashed contour); however, it should be approximately 5 mb deeper.

b. Surface flow

The July time-mean surface flow field as computed by the M-model is contrasted with its observed counterpart (Mintz and Dean, 1952) in Fig. 3.2. The surface flow field associated with the south Asian monsoon is a large-scale circulation extending over much of the Eastern Hemisphere and is characterized by divergent southeast flow emanating from the subtropical anticyclones of the Southern Hemisphere (30°S), becoming a southwesterly flow as it crosses the equator, and converging into the vicinity of the south Asian low pressure belt around 20–30°N. As this broad band of northward moving air crosses the equator and approaches the Indian subcontinent, large amounts of moisture and latent heat are supplied to it from the ocean surface. As a result, the large-scale circulation at the surface associated with the south Asian monsoon transports large amounts of moisture from the Southern Hemisphere to the Northern Hemisphere in July. Over the northern reaches of the Arabian Sea, this flow encounters the dry northwest Arabian flow. Over India and south Asia, this air flows eastward around the Himalayas. Finally, over eastern China, it moves north and westward into central Asia.

Imbedded in the large-scale circulation are smaller-scale features which are also important characteristics of the south Asian monsoon. For example, along the Abyssinian Highland off the east coast of Africa, a strong concentrated southerly flow, commonly called the Somali jet, is simulated by the M-model. Over the western Pacific, a line of convergence that roughly parallels the eastern coast of Asia reflects the path of a large number of tropical cyclones. Convergence into the monsoon trough is also simulated by the M-model; however, the convergence is not as strong as normally observed and the easterlies usually found to the north of the trough are also very weak.

c. Precipitation

Mean July precipitation patterns as computed by the M-model are contrasted with the mean June-July-August observed precipitation patterns of Möller (1951) in Fig. 3.3. In the vicinity of the south Asian monsoon, many of the features of the rainfall distribution reflect the characteristics of the flow field at the surface. For example, the region of confluence imbedded in the southwesterly flow extending from the equator southwest of India northeastward toward Burma is a region of maximum rainfall. A region of maximum rainfall is found in the southeast section of India with lesser amounts in northwestern India and the northern extents of the Arabian Sea, an area of minimum rainfall where dry northwest flow from Arabia persists. Along the track of tropical cyclones in the western Pacific is also a region of maximum precipitation.

The most striking discrepancies of the rainfall distribution as computed by the M-model are the lack of rainfall associated with the narrow mountain range in southwestern India (Western Ghats) and the lack of heavy rainfall over northeastern India in the Ganges River basin. As pointed out earlier, the imposed surface mountain heights were smoothed in space resulting in the lowering and broadening of the tall, narrow Western Ghats (Fig. 2.1). This probably explains the lack of orographically induced rainfall along the western coast of India.

But the Burma mountain ranges may have a more subtle influence that is not accurately simulated by the M-model because of its smoothed orography. Over northeastern India, simulated rainfall amounts are underestimated and the easterly flow along southern Tibet is weak. This may be due to at least a partial absence of the blocking effect of the Burma Mountains as described by Flohn (1968) and Banerji (1929, 1930). Flohn has gathered evidence that, as the southwesterly flow at the surface approaches the Burma Mountains to the north and east, it is forced into a counterclockwise curvature by the combined effects of the Burma and Himalayan mountain ranges. With low mountain heights prescribed for Burma in the M-model, part of the blocking effect may be absent, with moisture and latent energy being transported across the mountain range rather than being deflected westward over the Ganges river basin. Additional numerical simulation experiments designed to address this question are being conducted.

The principal precipitation agents observed over northeast India and northern Burma are the low pressure disturbances and monsoon depressions which form over the northern part of the Bay of Bengal (Ananthakrishnan and Bhatia, 1958). Typically, they slowly move to the northwest over northern India releasing large amounts of rainfall along their path. Such disturbances form in the M-model; however, they move northeastward over the Burma Mountains. The

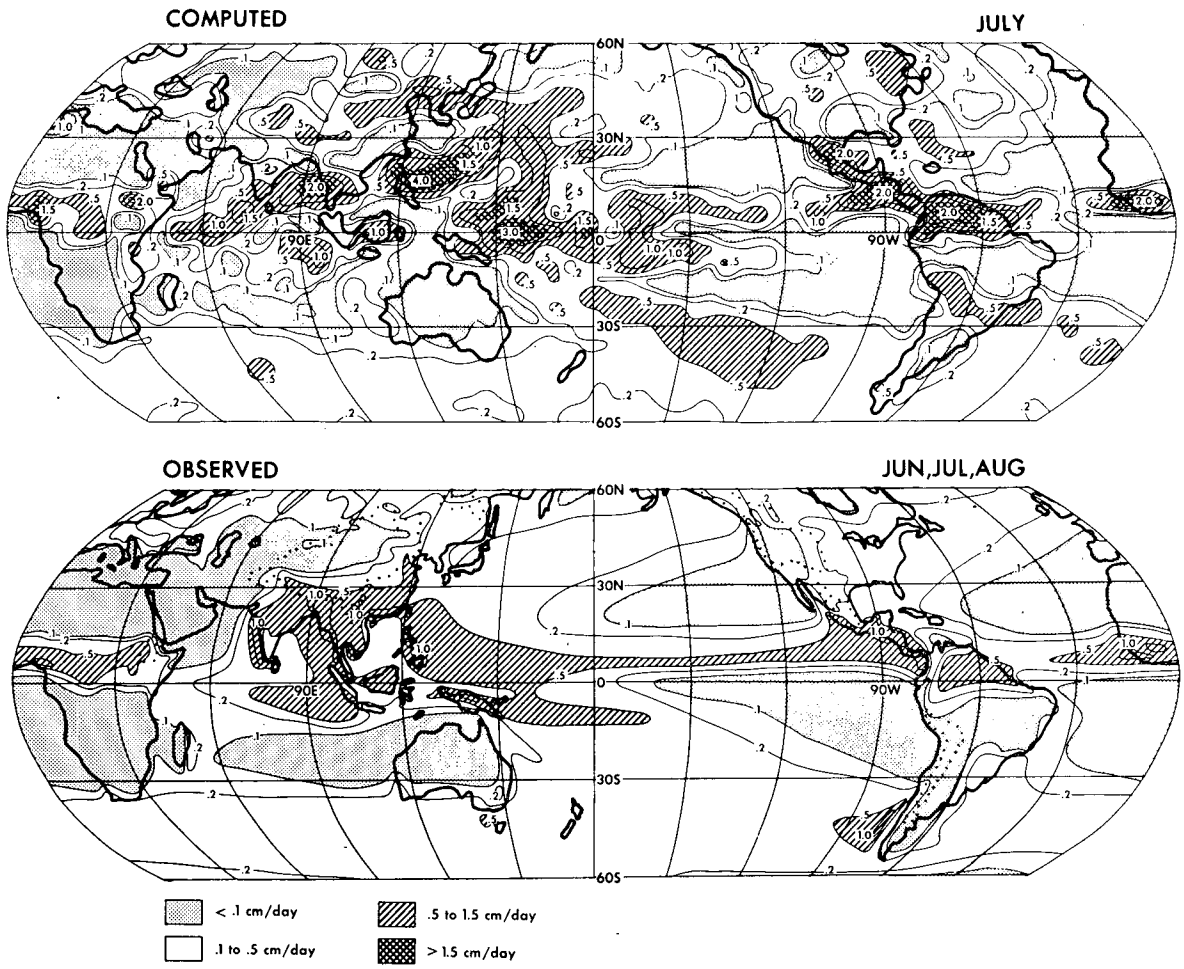

FIG. 3.3. Horizontal distributions of the time-mean rate of precipitation (cm day^{-1}). Top, computed July mean of the M-model; bottom, observed June-July-August mean (Möller, 1951).

atypical behavior of these disturbances may be related to the M-model's failure to simulate accurately the distribution of the flow responsible for steering them. As Fig. 4.3 indicates, the model underestimates the vertical extent of the easterly jet at 20°N and overestimates the thickness of the underlying layer of westerlies. Further investigation is required to confirm this speculation.

d. Upper tropospheric flow

Observations, as well as the M-model simulation, reveal the upper branch of the Hadley circulation that is associated with the south Asian monsoon (see Fig. 3.4). In the M-model, a strong easterly jet which extends over most of the Eastern Hemisphere dominates the circulation in the upper troposphere of the tropics. The easterly jet predominates only during the monsoon season and is responsible for transporting large amounts of mass and easterly momentum from the Northern Hemisphere into the Southern Hemisphere (see Manabe *et al.*, 1974).

Another dominant feature of the M-model simulation of the upper troposphere is the large-scale anticyclonic circulation located at 20–30°N, roughly over the warm core south Asian low pressure belt (compare Fig. 3.1). The large-scale anticyclonic circulation is the source region for air flowing southwestward into the Southern Hemisphere via the easterly jet. In the M-model, the center of the 190 mb anticyclonic circulation, as well as the easterly jet, are located about 5° too far south.

Over the western Pacific, a less extensive, somewhat unrealistic, anticyclonic circulation is maintained over a region where an excessive number of tropical cyclones persist in the M-model. The unrealistic anticyclonic circulation over the western Pacific modifies the circulation associated with the easterly jet.

e. Onset of monsoon

The time of onset of the monsoon is dependent upon which one of the various definitions of monsoon is accepted. According to the *Glossary of Meteorology*, the word monsoon was derived from the Arabic word

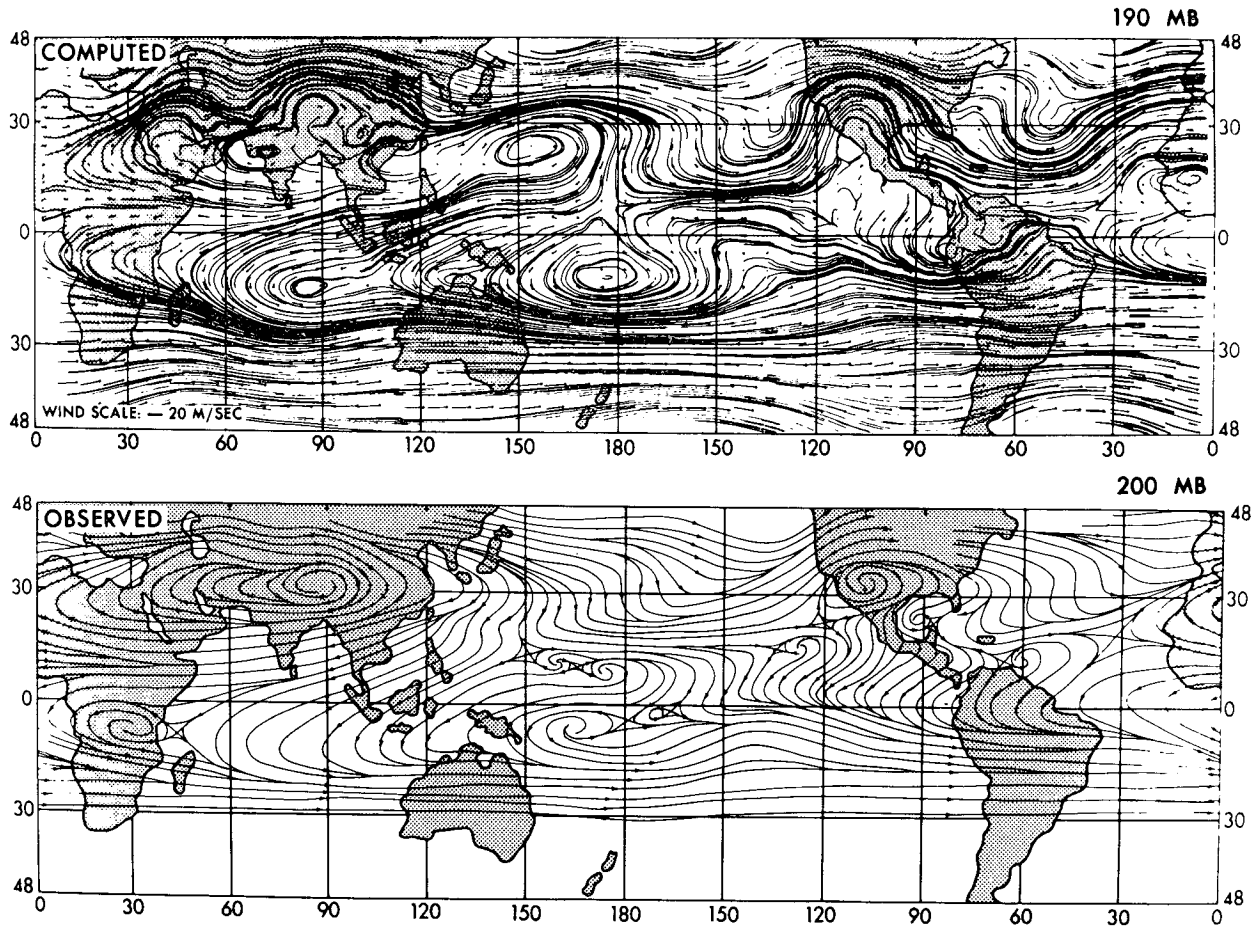

FIG. 3.4. Top, July mean vectors and streamlines at the 190 mb level of the M-model; bottom, observed streamlines at 200 mb (Sadler, 1972).

"mausim" which refers to seasonal winds. Applying this definition to the south Asian monsoon, the onset of the monsoon takes place when the lower tropospheric winds shift from the north and northeast to a south and westerly flow over the north Indian Ocean. However, in India the term monsoon is used only for the rainy period, and therefore, the onset is the time when heavy rainfall moves onto the Indian peninsula. It has been pointed out by many that the seasonal shift of prevailing winds does not necessarily correspond with the beginning of the rainy season. The shift of the surface winds may take place one and perhaps as much as two months before the commencement of copious rainfall over parts of India, while over southeastern Tibet the onset of the rainy season often takes place before the surface wind shift. Both the onset of southwesterly flow and the beginning of the rainy period often take place in an abrupt manner.

For the M-model simulation, onset of the wind shift from a northerly component to a southerly component in the vicinity of the Bay of Bengal is shown in Fig. 3.5, a latitude-time section of the 5-day mean meridional wind component averaged from 80°E to 95°E. The abrupt onset of the wind shift takes place from 26–30

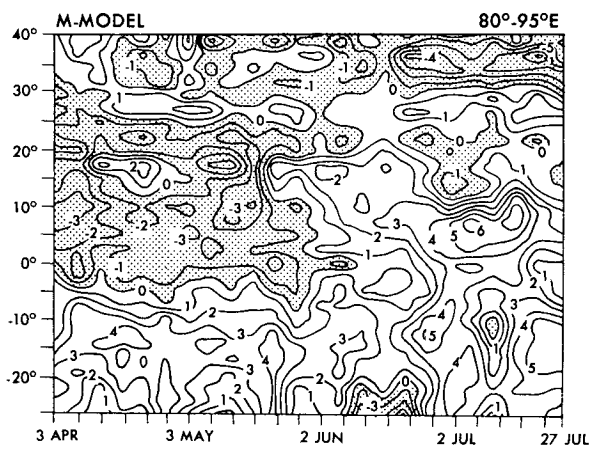

FIG. 3.5. Latitude-time section of zonally averaged (80–95°E) meridional wind (m s^{-1}) near the earth's surface ($\sigma = P/P_* = 0.99$) of the M-model.

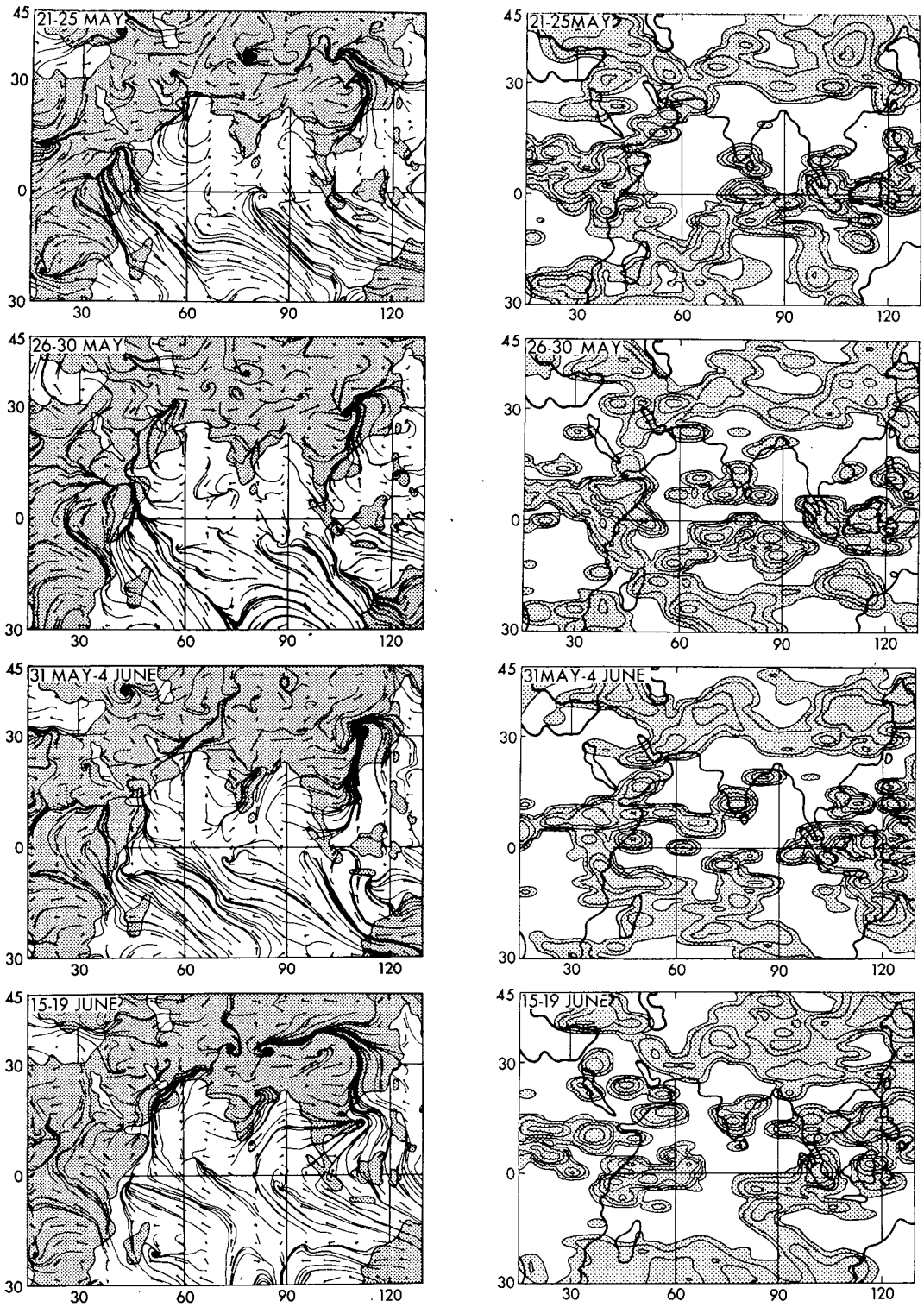

FIG. 3.6a. Five-day mean vectors and streamlines near the earth's surface ($\sigma = P/P_* = 0.99$) (left) and corresponding 5-day mean rate of precipitation (cm day^{-1}) (right) of the M-model. Contour values of rate of precipitation are 0.1, 0.2, 0.5, 1.0, 2.0, 5.0 cm day^{-1}. A wind vector of length 13° longitude represents a wind speed of approximately 20 m s^{-1}.

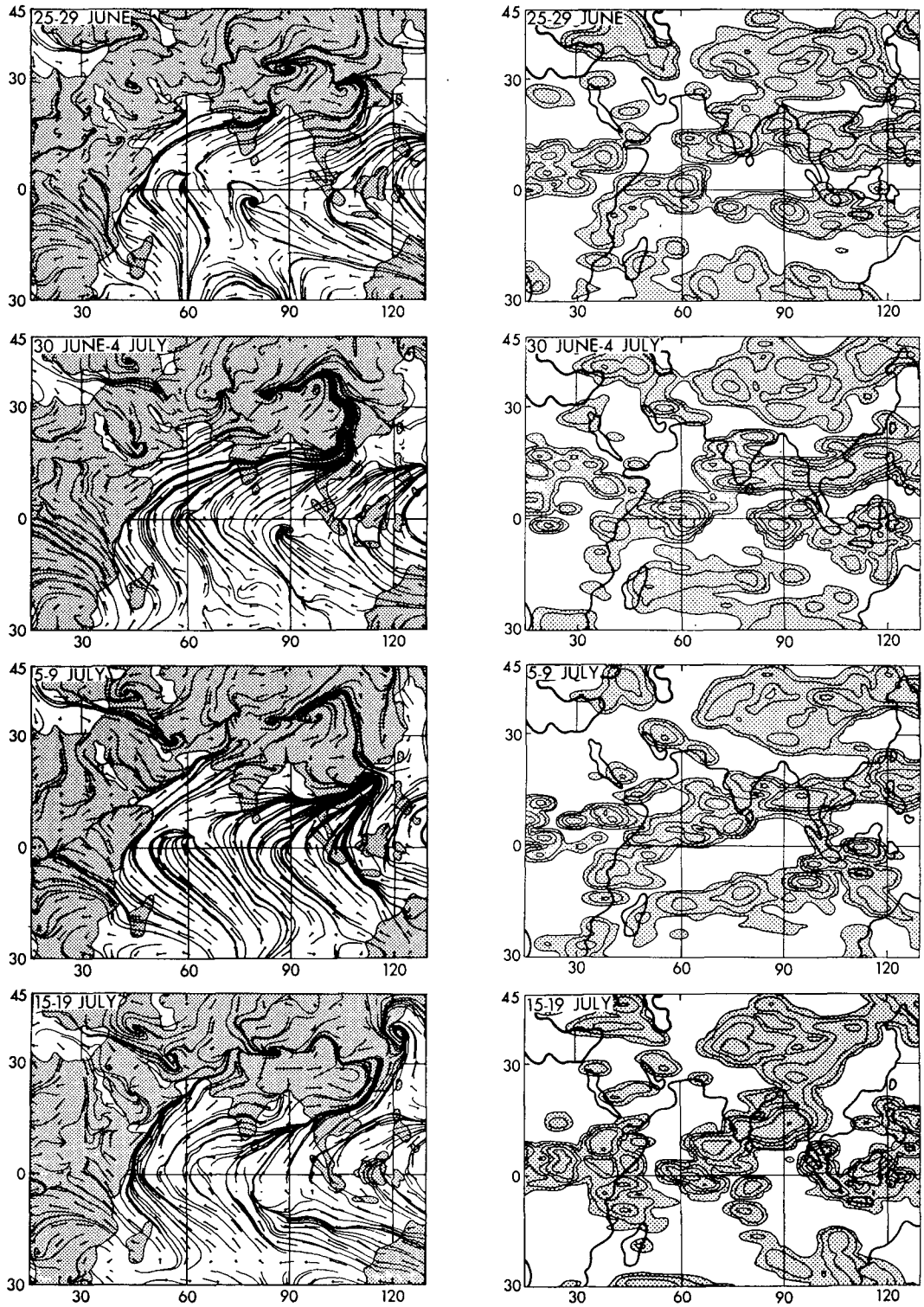

FIG. 3.6b. Same as Fig. 3.6a.

May, when most of the surface flow from 5°S to 30°N and 80°E to 95°E has a northerly component, to 31 May–4 June, when most of the surface flow in this region has a southerly component. A sequence of 5-day mean surface flow patterns and rainfall distributions which correspond in time to this event are shown in

Fig. 3.6. The M-model surface flow patterns over the north Indian Ocean for the 5-day periods 21–25 May and 26–30 May are very similar to the observed surface flow patterns which persist during the two months preceding the onset of the southwesterly flow (compare Ramage *et al.*, 1972). Flow patterns for the 21–25 May and 26–30 May periods are characterized by divergent flow toward the equator from a pair of anticyclonic cells over the Arabian Sea and the Bay of Bengal and southeasterly flow toward the equator in the south Indian Ocean, resulting in mass convergence along the ITCZ just south of the equator. As identified by the latitude-time section in Fig. 3.5, the onset of the southwesterly flow begins in the 31 May–4 June time period. Orgill (1967) pointed out that tropical depressions which form over northeastern India and the Bay of Bengal often usher in the southwesterly flow over Burma and the Bay of Bengal several days before the southwesterly flow appears at the surface over the Arabian Sea and the west coast of India. A similar circumstance appears in the M-model simulation. Southwesterly flow suddenly appears in the 31 May–4 June mean surface flow over the Bay of Bengal as the weak depression over northeastern India intensifies (Fig. 3.6a). Weak depressions over northeastern India persist through the 15–19 June time period, while southwesterly flow over the Bay of Bengal becomes more widespread, and onshore, northwesterly winds develop along the west coast of India. Also by 15–19 June, the Somali jet becomes established along the east coast of Africa as the heat low in northwestern India becomes more established. By 25–29 June as temperatures continue to rise over Tibet, southwesterly flow becomes established over the Arabian Sea as had been earlier established over the Bay of Bengal.

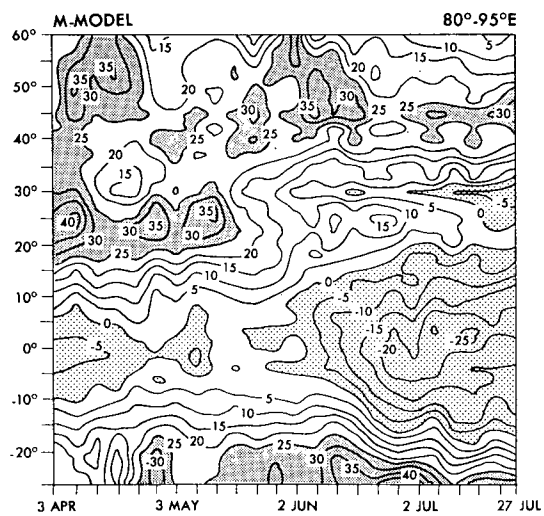

FIG. 3.7. Latitude-time section of zonally averaged (80–95°E) 5-day mean zonal winds (m s^{-1}) at the 190 mb level of the M-model.

Through the 25–29 June time period, it is important to note that convergence persists along the equator, and almost all of the southeasterly flow emanating from the subtropical high pressure belt around 30°S is confined to the Southern Hemisphere (except for the strong cross-equatorial flow associated with the Somali jet). Beginning with the 30 June–4 July time period, the convergence along the equator breaks down and much of the surface flow which converges over south Asia is associated with streamlines which originate in the subtropics of the Southern Hemisphere. This large-scale cross-equatorial flow pattern persists throughout most of July and provides a mean circulation which is able to transport additional moisture into the Northern Hemisphere.

The time of onset of the monsoon circulation for the M-model simulation is approximately 11 to 15 days later than the mean arrival date as observed by Orgill (1967). Orgill defined the onset to occur when the 10,000 ft equatorial shearline fractured or changed orientation and allowed equatorial westerlies to extend north of 15°N. Based upon this criterion, he determined the dates of onset from 1936 through 1964, and found the earliest onset date to be 1 May, the latest 3 June, and the mean 20 May. For the M-model, a similar analysis was done on the surface flow (not at 10,000 ft) and Figs. 3.5 and 3.6 indicate that surface equatorial southwesterly flow first extends north of 15°N over the Bay of Bengal in the 31 May–4 June time period. In previous years of the M-model experiment, the onset of the monsoon circulation took place at earlier dates. It is not clear whether interannual variations in the onset of the monsoon circulation are due to a transient behavior of the model resulting from a thermal imbalance of initial conditions, or whether they are due to the natural variability of the model itself. Analysis of a much longer time integration of the model is necessary to resolve this question.

The abrupt onset of the monsoon circulation at the surface is often related with the abrupt northward shift of the jet stream. In the vicinity of the Tibetan Plateau, the presence of the mountain range has an important effect on the flow patterns at levels much higher than the mountains themselves. Yin (1949) suggests that the burst of the monsoon begins when the subtropical jet abruptly shifts northward from a path along the southern periphery of the Tibetan Plateau to a path along the northern periphery. Fig. 3.7 is a time section of the zonal wind component at 190 mb of the M-model simulation. About 20–25 May, the subtropical jet (at about 25°N) rapidly weakens and an intensified zonal flow appears at about 40–45°N. This is evidence of the abrupt shift of the jet stream to the northern periphery of the Tibetan Plateau in the M-model simulation. Soon after this event, the abrupt onset of southerly flow takes place over eastern India and the Bay of Bengal. These two events are probably closely related

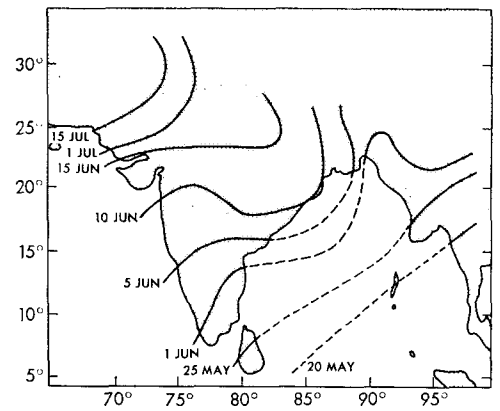

FIG. 3.8. Observed normal dates of onset of monsoon rainfall (From Ananthakrishnan and Rajagopalachari, 1964).

as Yin suggested, and it also indicates that the Tibetan Plateau may be instrumental in causing the onset to be quite abrupt. Results from the experiment without mountains, presented in Section 5, will address this question further.

It often takes until mid-July before maximum rainfall sets in over all of India, four to six weeks after the initial appearance of southwesterly flow. Unlike Orgill, who defined the onset of the monsoon as corresponding to the time that the wind shifts, Ananthakrishnan and Rajagopalachari (1964) defined the onset of the monsoon using rainfall measurements. Fig. 3.8 shows the normal dates of onset of the monsoon rainfall over India and the Bay of Bengal, as computed by Ananthakrishnan and Rajagopalachari using 50 years of rainfall measurements. In general, this figure shows that the advance of the monsoon rainfall is from southeast to northwest over India, with monsoon rainfall beginning near the end of May in southeast India, gradually migrating northwestward until mid-July when monsoon rainfall begins in northwest India.

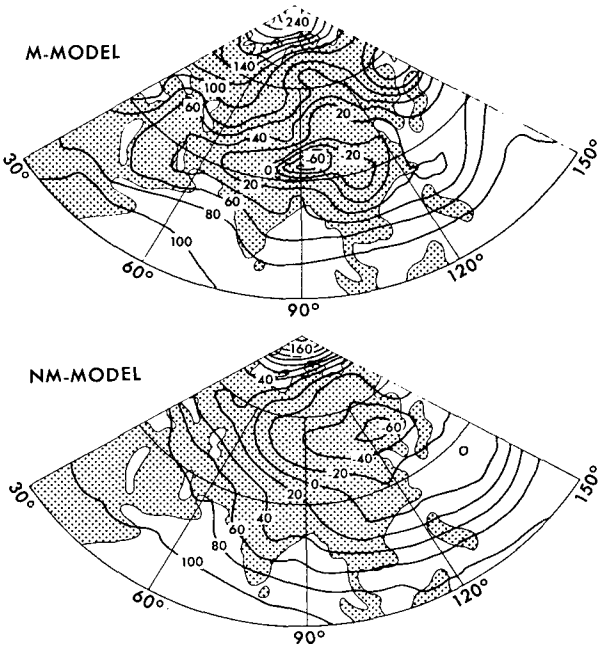

FIG. 4.1. Horizontal distributions of July mean geopotential height (m) of the 1000 mb surface. Top, M-model; bottom, NM-model.

In the M-model simulation, a similar migration of rainfall patterns takes place during the onset of the monsoon (Fig. 3.6). For the 21–25 May and 26–30 May means, pre-monsoon precipitation occurs over southern India and northeast India, regions where pre-monsoon rainfall is prevalent from March through May. Beginning with the 31 May–4 June time period when southwesterly flow commences to flow over the Bay of Bengal, rainfall exists along the south and east coasts of India. The rainfall patterns expand northward and westward for the 15–19 June and 25–29 June time periods lagging approximately 10–15 days behind

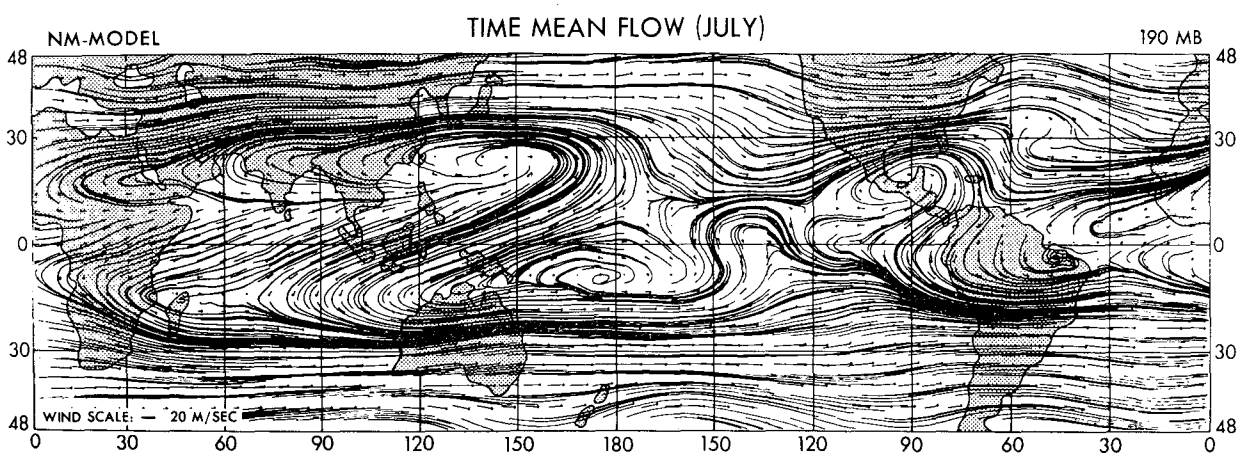

FIG. 4.2. July mean vectors and streamlines at the 190 mb level of the NM-model.

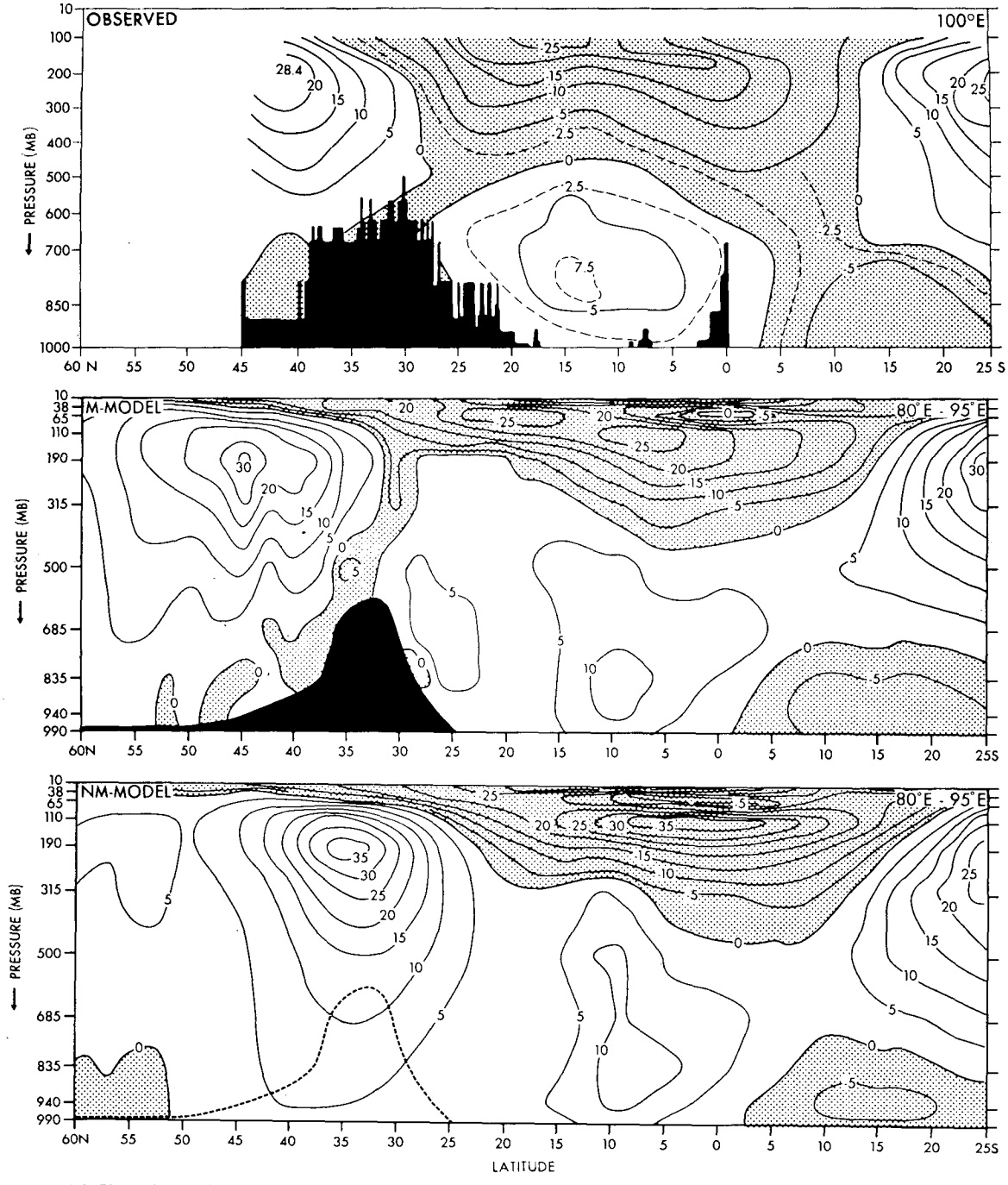

FIG. 4.3. Top, observed latitude-pressure distribution of July mean zonal wind (m s^{-1}) along 100°E from Ramage (1971). Middle, computed latitude-pressure distribution of July mean zonally averaged (80–95°E) zonal wind (m s^{-1}) for the M-model. Bottom, same as middle for the NM-model.

the normal arrival dates of Ananthakrishnan and Rajagopalachari.

4. Manifestations of mountain effects on the monsoon

a. South Asian low

The effect of mountains on the large-scale monsoon circulation over south Asia in July is illustrated in Fig. 4.1 which shows the July time-mean 1000 mb geopotential height maps for the M-model and the NM-model. In the NM-model, the continental low is located at about 50°N, 125°E, far to the north and east of the low pressure belt in the M-model experiment which is centered around 30°N with lowest pressure located near the highest point of the Himalayas.[1] This

[1] It is possible that the low results mainly from the large extrapolation downward to the 1000 mb surface in the mountain region. However, Fig. 4.7 indicates that a region of low pressure does exist over the Himalayas.

indicates that mountains have an important effect on the large-scale south Asian monsoon circulation in that they provide mechanical and/or thermodynamical effects which maintain a low pressure belt in their midst, much nearer the equator than the low pressure system that develops in the NM-model which has only the effects of land-sea contrast. As a result, in the subtropics of the Northern Hemisphere of the NM-model, geostrophic flow near the surface is northwesterly, a circulation which inhibits sea-to-land flow from penetrating far into Asia at the surface. Another effect of the Asian continental low being located far to the northeast in the NM-model is the decreased south-to-north pressure gradient (30°S to 30°N), particularly in the western regions of the monsoon circulation.

b. Upper tropospheric flow

In the upper troposphere, almost all of the primary circulation features of the M-model (Fig. 3.4) are also circulation features of the NM-model (Fig. 4.2). For the circulation in the Eastern Hemisphere that is an integral part of the monsoon circulation, the main effect of mountains is to move the center of the south Asian anticyclone from a latitude south of the Himalayas in the NM-model to a location (approximately 30°N, 90°E), closely corresponding to the highest moutain peaks of Tibet in the M-model (compare Fig. 3.4). The upper tropospheric anticyclone lies almost directly over the south Asian low at the surface and the highest mountains in the M-model; however, in the NM-model the upper tropospheric anticyclone lies to the south of Tibet and the surface low lies far to the northeast of Tibet. This result tends to confirm the fact that mountains play an important role in the south Asian monsoon circulation, and that a complete description of the monsoon circulation involves more than a discussion of the contrasting thermal properties of the vast Asiatic land mass with that of oceanic regions to the south.

c. Zonal wind

North-south cross sections at longitudes 80–95°E corresponding to the region of highest mountains in Tibet clearly depict the effects of mountains on the zonal mean state of the atmosphere in the south Asian monsoon region. Fig. 4.3 shows the mean zonal wind averaged over this region for both the M-model and the NM-model in July. Compared to results from the NM-model, both the westerly and easterly jets are weaker in the M-model, and their centers are displaced approximately 10° to the north. Directly over the mountains in the M-model, in place of the westerly jet of the NM-model, a tongue of weak easterly flow extends from the surface to the stratosphere where strong easterly flow predominates. From the mountains southward to the equator in the troposphere of the M-model, westerly flow prevails except for a small region of easterly flow adjacent to the south side of Tibet. In the lower troposphere from 15°N southward

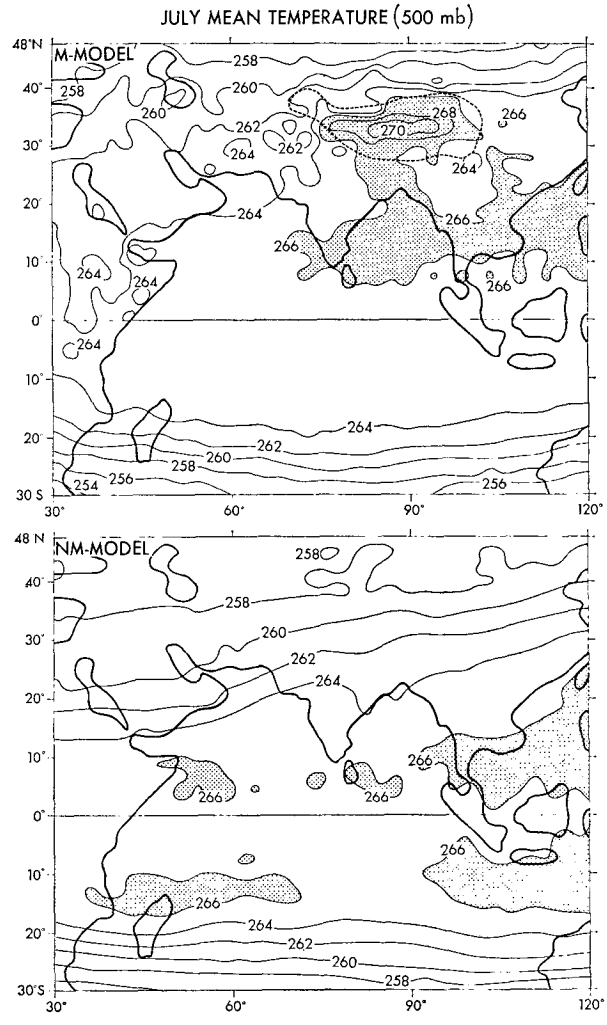

FIG. 4.4. Horizontal distribution of July mean 500 mb temperatures (K) of the M-model (top) and the NM-model (bottom).

where few mountains exist, zonal wind profiles of both models are similar. The zonal wind profile of the M-model is in close agreement with the observed zonal wind profile along 100°E (Ramage, 1971), with the most notable exceptions being that the upper tropospheric easterly flow of the M-model does not extend as far downward into the middle troposphere at 20°N and easterly flow does not extend from the stratosphere all the way down to the surface in the Southern Hemisphere.

d. Temperature

The July time-mean 500 mb temperatures for both the M-model and the NM-model are shown in Fig. 4.4. In the model with mountains, maximum 500 mb temperatures are found over the Tibetan Plateau (none of the smoothed mountain heights reach 500 mb) with a secondary maximum to be found at 15°N over the Bay of Bengal and eastward. The location of maximum 500 mb temperatures in the M-model agrees quite

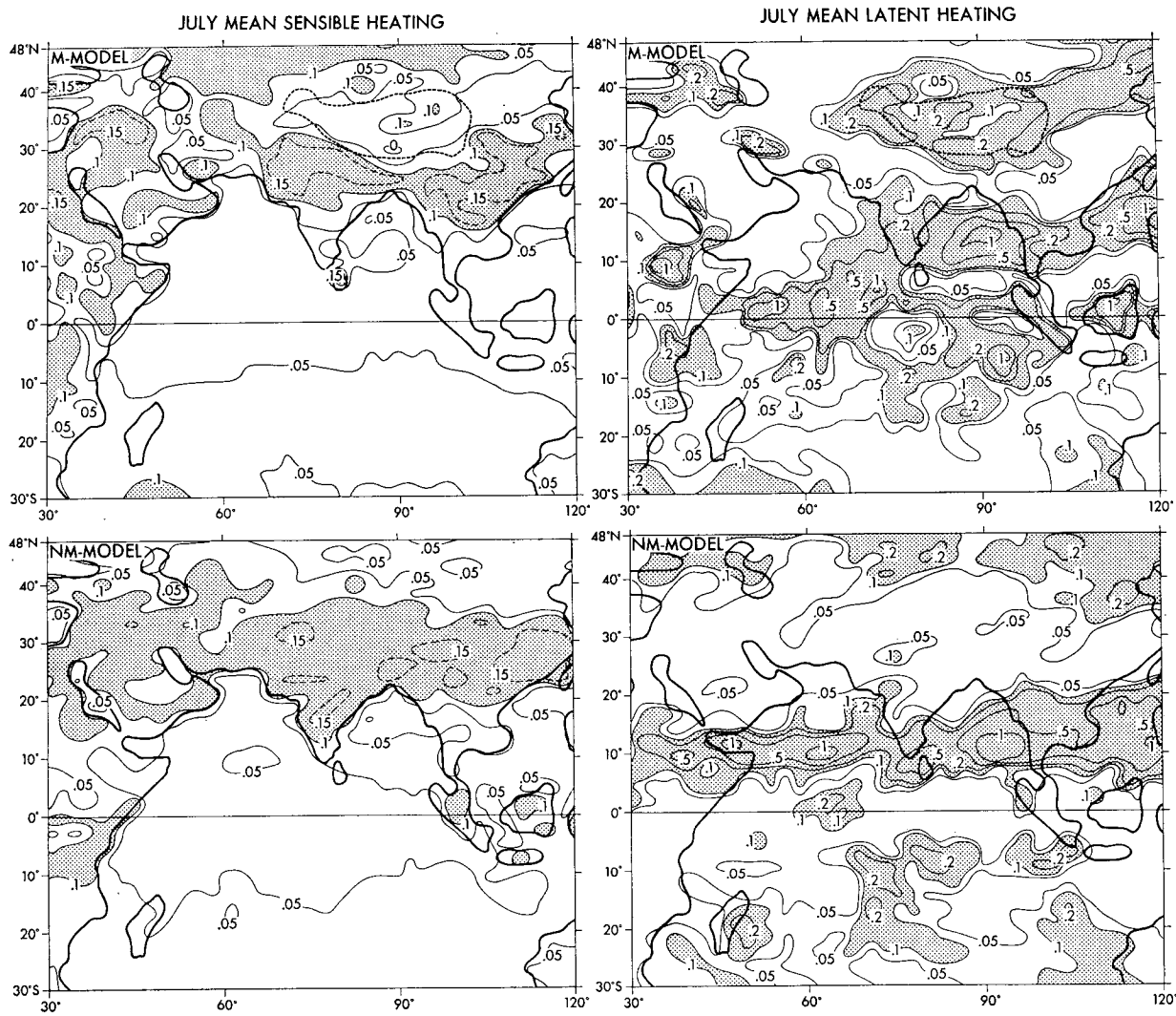

FIG. 4.5. Left, horizontal distributions of July mean sensible heating of the atmosphere by the earth's surface (ly min^{-1}). Right, horizontal distributions of July mean, vertically integrated rate of latent heating of the atmosphere (ly min^{-1}). Top, for the M-model; bottom, for the NM-model.

well with the observational findings of Flohn (1968). In the NM-model, temperatures over Tibet are approximately 10–12°C lower than in the M-model with maximum temperatures located along a line from east of Africa at 5–10°N extending eastward into the western Pacific. Evidence clearly exists that a mid-tropospheric heat source is maintained over the mountains in the M-model, and that it contributes to the formation of the warm core low pressure area (Fig. 4.1) which lies over the mountains of Tibet.

Two primary effects often cited for maintaining high temperatures over the mountains are sensible heating of the air arising from a summer surplus of solar energy absorbed at the earth's surface in the vicinity of the mountains, and latent energy released by orographic uplifting of moist air along the mountain slopes. The mean July horizontal distributions for sensible heat flux from the earth's surface and vertically integrated latent heating are shown for the M-model and the NM-model in Fig. 4.5. Clearly, the most significant difference in the heating fields of these two numerical simulations is that latent heating tends to be most important over Tibet in the M-model, while sensible heating tends to dominate there when mountains are removed. In both models, the regions of highest mid-tropospheric temperatures correspond quite closely to regions of maximum latent heat release, and over the mountains of Tibet, the role of sensible heating by the earth's surface actually becomes less significant when mountain effects are incorporated. This tends to support some of the skepticism of Rangarajan (see Introduction) about the role of sensible heating in the monsoon circulation. Maximum rates of sensible heating over arid regions of both models are about

equal; however, in the NM-model, the region of maximum sensible heating rates covers a much wider area, approximately coinciding with the location of the large-scale south Asian low pressure belt in the M-model. Even with this added help, a south Asian low pressure belt does not form in the NM-model. Therefore, we must conclude that maintenance of the warm core south Asian low in the M-model is dependent on the latent heating induced by mountain effects.

The horizontal fields of 500 mb level vertical velocity for both the M-model and the NM-model are shown in Fig. 4.6. For the NM-model, this field is very simple, resembling the vertical velocity field corresponding to simple Hadley cells surrounding an ITCZ, with broad bands of descending motion both to the north and south of a narrow band of intense upward motion oriented roughly east-west and centered about 10°N. At the 500 mb level of the M-model, vertical velocity patterns are more complex with regions of upward motion corresponding to regions of maximum latent heating.

In terms of understanding the thermal effects of the mountains at 500 mb, the most interesting descending motion regions are those which lie along the periphery of the Tibetan Plateau in the M-model. Adiabatic warming of descending air along a band surrounding the mountains may be an important mechanism for explaining warm temperatures in the middle troposphere south of Tibet where latent heating is minimum. Over northern India this narrow band of descending motion corresponds to the region of the monsoon trough.

In order to show the effects of thermal processes at a longitudinal belt intersecting the Tibetan Plateau, contrasting profiles of temperature deviation are shown in Fig. 4.7. Temperature deviation, $T'(\theta,P_n)$, is defined by

$$\left.\begin{aligned} T'(\theta,P_n) &= \overline{T(\theta,\lambda,P_n)}^{\lambda} - A(P_n) \\ A(P_n) &= \tfrac{1}{2}\left[\overline{T_M(\theta,\lambda,P_n)}^{\lambda\theta} + \overline{T_{NM}(\theta,\lambda,P_n)}^{\lambda\theta}\right] \end{aligned}\right\},$$

where λ is longitude, θ latitude, $\overline{(\ )}^{\lambda}$ and $\overline{(\ )}^{\theta}$ indicate averaging over the longitudinal range 80–95°E and the latitudinal range 25°S–60°N respectively, T_M and T_{NM} are temperature in the M-model and the NM-model respectively, and P_n the normalized pressure[2] is obtained from

$$P_n = P \times (P_{1000}/P_{GSL}),$$

where P_{1000} is the 1000 mb pressure and P_{GSL} the global mean sea level pressure. Fig. 4.7 indicates that much higher temperatures are maintained in the middle troposphere over Tibet when effects of mountains are included; however, near the surface, higher temperatures are maintained when effects of mountains are neglected.

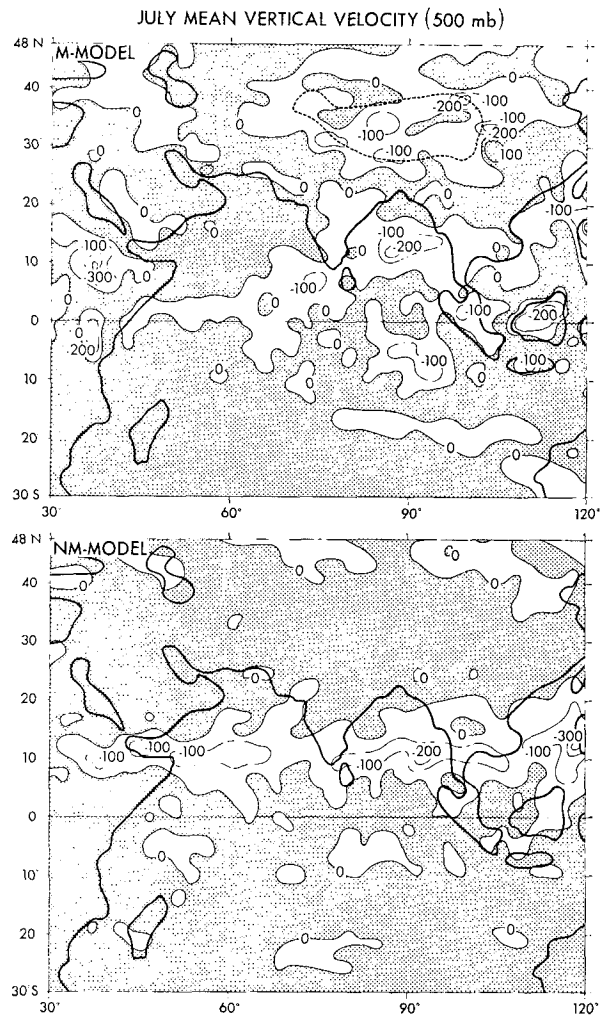

FIG. 4.6. Horizontal distribution of July mean vertical velocity (mb day^{-1}) at the 500 mb level of the M-model (top) and the NM-model (bottom).

Primarily due to the effect of much more latent heating over the Tibetan Plateau region in the M-model than in the NM-model in July, the warm layer over Tibet extends to higher levels in the M-model. Fig. 4.7 also shows a profile of the resulting geopotential deviation computed in the same way as temperature deviation. As a result of the deep layer of high temperatures over Tibet during July, a low pressure envelope is created over the mountains in the M-model, and it extends southward over the plains and the Bay of Bengal, a feature not found in the NM-model. Accordingly, the large-scale surface pressure gradient from 30°S to the mountains of Tibet is stronger in the M-model which gives rise to a positive feedback mechanism: high temperatures over Tibet give rise to

[2] Since the total mass of the M-model atmosphere is chosen to be the same as that of the NM-model atmosphere, the global mean sea level pressure of the former (1013 mb) is larger than that of the latter (988 mb) due to orography. In order to reduce a bias caused by this difference, normalized pressure is used as a vertical coordinate for constructing the deviation fields in Fig. 4.7.

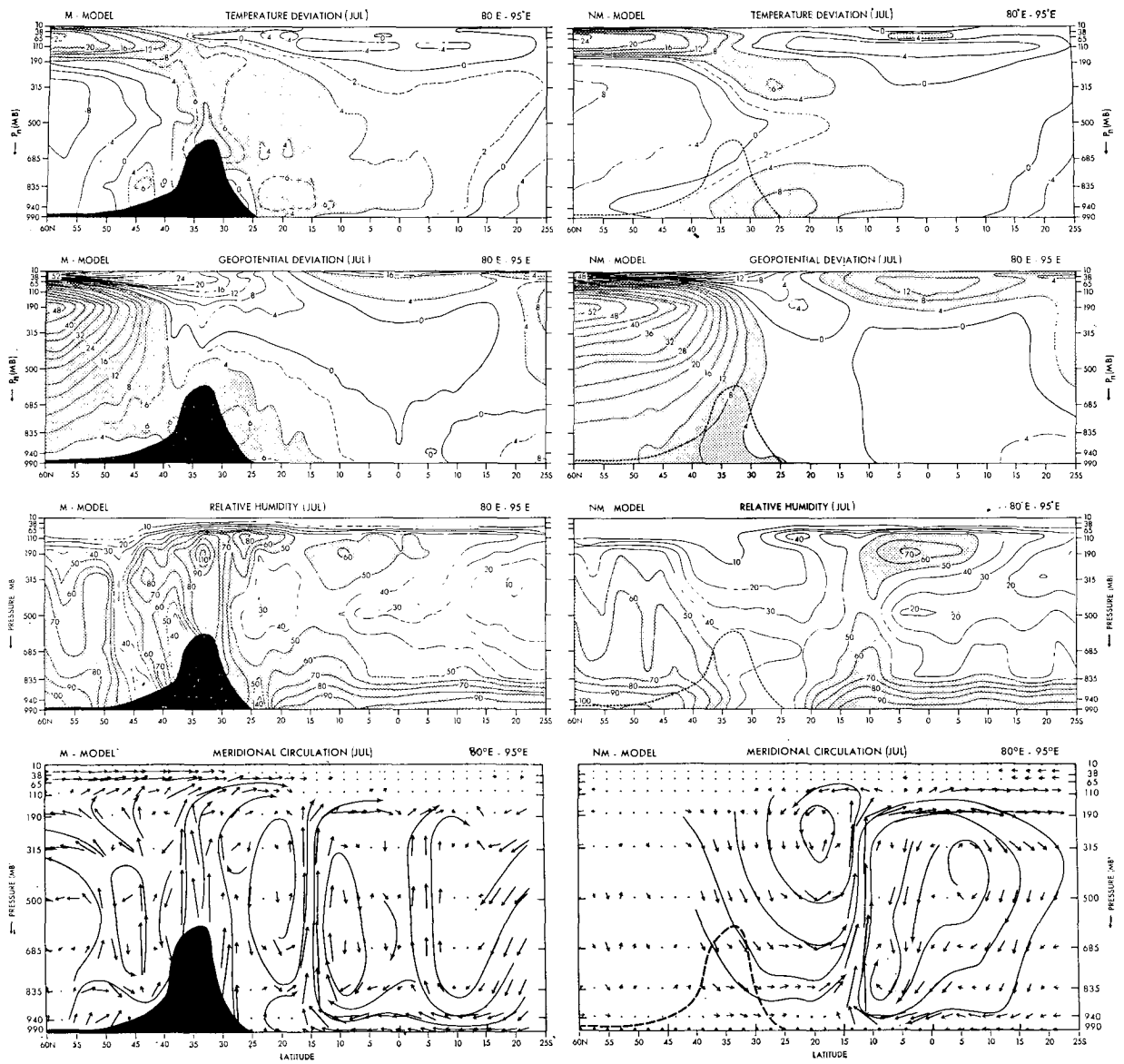

FIG. 4.7. Distributions of various July mean fields zonally averaged from 80–95°E for the M-model (left) and the NM-model (right). Top, temperature deviation (K); second from top, geopotential height deviation (×10 m); third from top, relative humidity (percent); bottom, meridional circulation. Relative humidity was calculated from July mean fields of mixing ratio and temperature; therefore, values above 100% are encountered.

lower pressure in this region yielding stronger south-to-north pressure gradients and more convergence in the vicinity of the mountains, which results primarily in more latent heat release and higher temperatures.

The effect of latent heating over the Tibetan Plateau on the circulation in the upper troposphere is also revealed in the geopotential deviation profiles. With high temperatures extending into the upper troposphere over Tibet in the M-model, the warm core south Asian low hypsometrically builds into a warm core anticyclone with increasing height; this is revealed in Fig. 4.7 by the positive geopotential deviations over the Tibetan Plateau in the upper troposphere. For the NM-model with relatively colder temperatures over Tibet, the warm core upper tropospheric anticyclone and positive geopotential deviations are shifted equatorward toward higher temperatures. These manifestations indicate that mountain effects modify the large-scale pressure distributions associated with the south Asian monsoon in a way that makes the region of the Tibetan Plateau a center of action at all tropospheric levels.

e. Meridional circulation

For both the M-model and the NM-model, Fig. 4.7 shows July mean relative humidity and meridional

circulation profiles averaged over the longitudinal section corresponding to the highest mountains. The most similar features of both meridional circulation cross sections are the two Hadley cells surrounding an ITCZ located at 15°N in the M-model and at 12°N in the NM-model. In the NM-model, over most of south Asia from the mountain region (region where mountains would exist if their effect were included in the NM-model) southward to the ITCZ, the meridional circulation is dominated by the descending branch of the northern Hadley cell where adiabatic warming serves to maintain a dry atmosphere (mean relative humidity less than 50%). In July in the M-model, the effects of mountains initiate upward motion in their midst in a region where descending motion exists in the NM-model. Accordingly, the area of dry descending motion is considerably smaller in the M-model, not only restricted horizontally to a narrow latitudinal belt by the two pillars of moist upward motion over the mountains of Tibet and along the ITCZ at 15°N, but also restricted vertically as dry descending motion at approximately 20–25°N extends downward only as far as the 835 mb level, with weak southerly flow and rising motion near the monsoon trough replacing dry descending northerly flow of the NM-model. Moist southerly flow at the surface in the M-model, passing northward beyond the ITCZ toward the mountain region, is much stronger over the Arabian Sea; longitudes selected for this cross section correspond to eastern India and the Bay of Bengal.

These contrasting meridional circulation and relative humidity profiles give further insight into the effect mountains have on the thermal structure of the south Asian monsoon. With an intense northern Hadley cell in the NM-model, south Asia is dominated by dry descending motion at all tropospheric levels, and the rate of temperature decrease with height is very large, approaching the dry adiabatic laspe rate. At the surface in the NM-model, southerly flow extends from the subtropics of the Southern Hemisphere northward to the ITCZ. In the M-model, this feature which transports moisture into the monsoon region extends even farther north to the mountain region. Therefore, when the effects of mountains are included, the atmosphere over south Asia is significantly more humid, and rising motion, latent heating, and moist adiabatic lapse rates tend to be more prevalent. As a result, temperatures tend to be higher in the middle troposphere and lower in the lower troposphere over south Asia when effects of mountains are included, and conversely, temperatures tend to be lower in the middle troposphere and higher in the lower troposphere over south Asia when effects of mountains are neglected.

Observed relative cloud cover for July based on three years of data from meteorological satellites (Miller, 1971, p. 66) reveals that the Tibetan Plateau is enshrouded with cloud cover during July with a band of heavy cloud cover persisting along the southern slopes of the mountains. Results from these two numerical experiments indicate that these features are dependent upon the effect of orography as upward cloud-producing motion over the Tibetan mountains in the M-model is replaced by a deep layer of sinking motion when the effect of mountains is removed. The July mean cloudiness field also indicates that a narrow belt of less intense cloud cover parallels the Tibetan Plateau south of the mountains along the monsoon trough. At longitude 90°E, minimum cloud intensity is found around 27°N with cloud intensity increasing equatorward to a maximum around 12–18°N. Instantaneous satellite cloud pictures, such as shown by Ramage (1971, p. 196), often show this band of relatively cloud-free area to be dotted with cumulus towers, and it is sometimes somewhat broader even during periods of a very active monsoon. The location of the narrow band of minimum observed cloud intensity corresponds approximately to the location of the narrow band of sinking motion south of the mountains in the M-model, and the location of maximum cloud intensity (90°E, 12–18°N) corresponds to the location of the ITCZ (12–15°N) in both numerical simulations.

f. Surface flow and precipitation patterns

As previously discussed, one of the most important effects of mountains on the south Asian monsoon circulation in July is that they help to maintain a heat source in the troposphere resulting in a low pressure envelope over the mountains which extends southward over the plains. The south Asian low pressure belt centered along 30°N in the M-model is entirely absent in the NM-model in July. Consequently, the south-to-north pressure gradient is substantially weaker in the NM-model, particularly in the western regions of the Arabian Sea. The broad band of moist southerly flow at the surface, emanating from the subtropical high pressure belt at 30°S of both models (Fig. 5.1, bottom), penetrates northward only as far as the latitude of the ITCZ in the NM-model, whereas partly because of the assistance of the south Asian low pressure belt, some of the southerly flow is able to pass all the way northward to the mountains of Tibet in the M-model in July.

In the surface flow field (Fig. 5.1, bottom), the ITCZ can be located at approximately the latitudes 10–15°N for both models in July. In the NM-model, the ITCZ at the surface is clearly identified by a line of convergence where northwesterly flow from Asia meets the maritime southwesterly flow originating in the Southern Hemisphere. In the M-model the characteristics of the ITCZ are somewhat different. It is identified by a line of confluence (rather than convergence) imbedded in the maritime southwesterly flow. From about 5°N over the Arabian Sea, the line of confluence extends northeastward across the southern tip of India, the Bay of Bengal, Burma, and eastern China. Upward from 835 mb in the M-model, the ITCZ is defined by a region of convergence where northerly flow meets

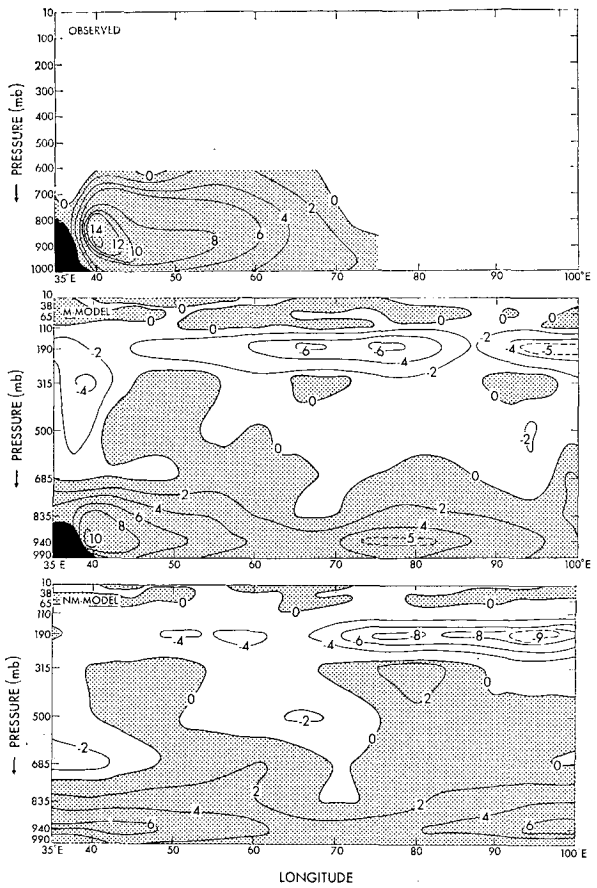

FIG. 4.8. Longitude-pressure distributions of July mean meridional wind (m s^{-1}) at the equator. Top, observed distribution redrawn from Findlater (1969); middle, M-model distribution; bottom, NM-model distribution.

flow with a southerly component, characteristics similar to those of the ITCZ in the NM-model (see Fig. 4.7).

The definition and characteristics of the ITCZ in the M-model are not in conformity with most other ideas put forth about the ITCZ in the monsoon circulation. Heretofore, the ITCZ and the monsoon trough have usually been considered as one and the same feature. However, there is some observational evidence that the simulated line of confluence along the ITCZ in the M-model is quite realistic. In an isotach analysis of observed July mean 850 mb wind fields (Ramage and Raman, 1972), a local maximum of mean wind speed is found to coincide with the position of the ITCZ in the M-model, particularly over the Bay of Bengal. Along the ITCZ in the M-model simulation, maximum upward motion is also found over the Bay of Bengal, with a secondary maximum along the ITCZ southwest of India and a tendency for downward motion east of south India (Fig. 4.6). Observed July mean cloudiness (Miller, 1971, p. 66) also tends to correspond to the M-model's simulated vertical motion patterns along the ITCZ. In addition, fields of monthly mean equivalent blackbody temperatures obtained from satellite data (Ramage *et al.*, 1972) indicate that clouds tend to extend to higher levels in the preferrred regions of upward motion along the ITCZ simulated by the M-model.

It should also be noted that the ITCZ is not a stationary feature of the M-model simulation. In 5-day mean streamline analyses (Fig. 3.6), the region of confluence in the surface flow is found to be oriented roughly east-west at 15°N over India during 30 June–4 July; later during 15–19 July, it is found just south of India oriented more northeast-southwest. The time-varying aspects of the ITCZ in the M-model will be further discussed in Section 5.

Located just east of the Abyssinian Highland, the Somali jet is a surface flow feature which is of great interest, as its strong concentrated southerly flow is responsible for transporting large amounts of moisture and latent energy across the equator into the south Asian monsoon region. Fig. 4.8 shows cross sections of the Somali jet as simulated by both models and as observed by Findlater (1969). In the M-model, the position of the Somali jet is well simulated; however, it is somewhat weaker than observed. Comparison of the two model simulations indicates that mountain effects contribute to making the Somali jet more intense, with the region of maximum southerly flow in the M-model confined to a narrower longitudinal belt (centered at 40°E). A more detailed analysis of the mechanical and thermodynamical effects of mountains (particularly the Abyssinian Highland) on the Somali jet is not yet completed.

Horizontal distributions of the mean precipitation rate in July for both models may be deduced from the latent heating distributions in Fig. 4.5. [Multiply latent heating rates (ly min^{-1}) by 2.4 for rate of precipitation in cm day^{-1} or by 0.945 for values in inches day^{-1}.] In both models, a rainbelt roughly corresponds with the position of the ITCZ. Since these features exist in both models, they do not owe their existence to mountain effects. However, their position may be influenced by the distribution of sea surface temperatures. In both models in July, the rainbelt and associated ITCZ are particularly well-defined over the Bay of Bengal where maximum sea surface temperatures are specified (Fig. A1). A tendency for coincidence of the rainbelt, the ITCZ, and the region of maximum sea surface temperature was previously studied by Manabe *et al.* (1974).

The most significant difference in the precipitation patterns between the two models is found north of the ITCZ. In the NM-model, a desert-like climate is simulated in south Asia resulting from dry northwesterly continental air flowing southward toward the rainbelt. However, in the M-model, moist southwesterly flow at the surface moves northward toward the

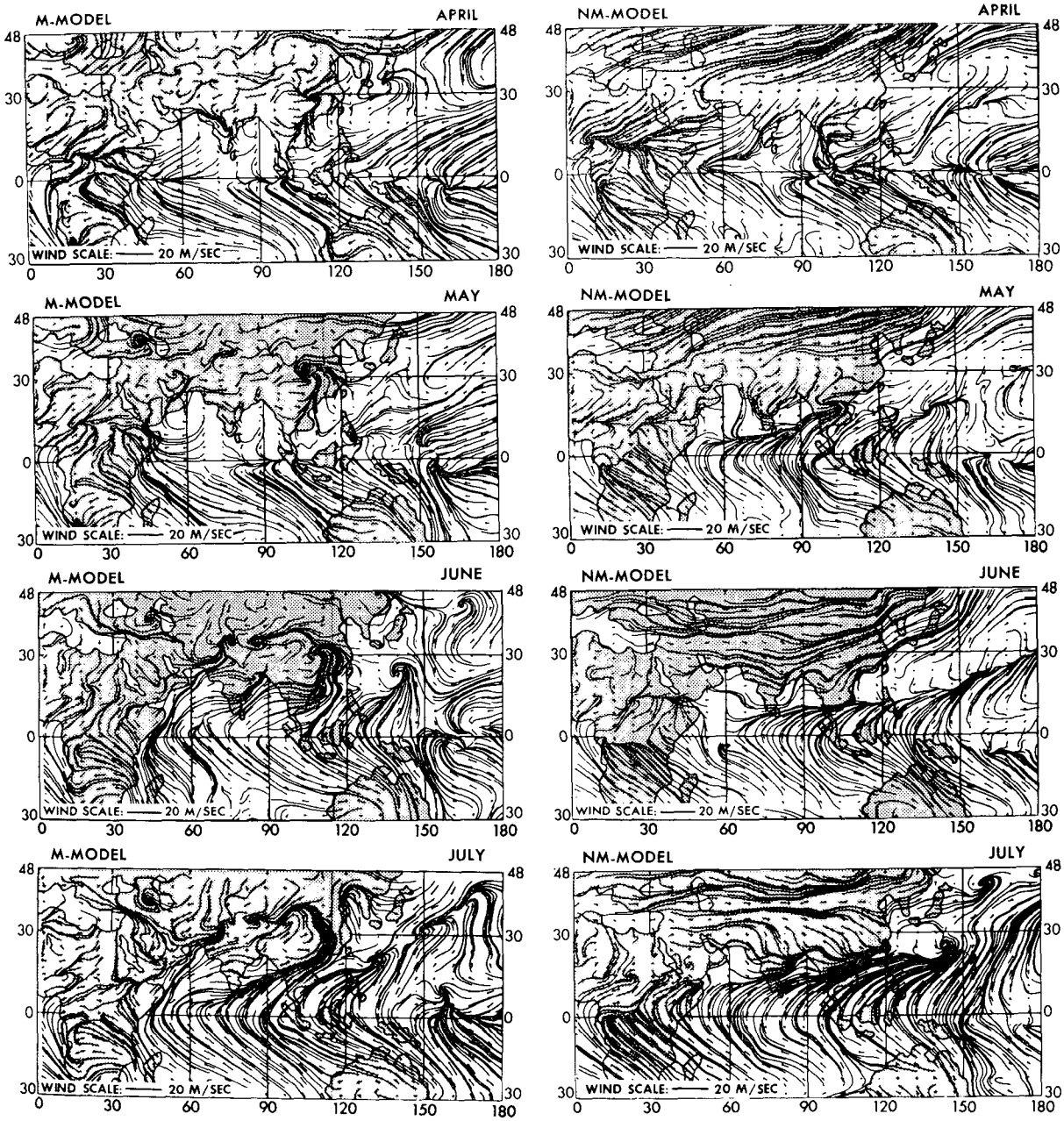

FIG. 5.1. Monthly mean vectors and streamlines for the M-model (left) and the NM-model (right).

south Asian low pressure belt, resulting in substantially more rainfall over south Asian continental regions. Larger amounts of rainfall are found particularly along the slope of the Tibetan Plateau with most of India receiving more rainfall than in the NM-model in July. As already discussed in Section 3, even more rainfall could be expected along the west coast of India and over northeastern India if the tall, narrow mountain ranges (Western Ghats and Burma mountains) had been more realistically resolved.

5. Effect of mountains on the onset and evolution of the monsoon

a. Surface flow and sea level pressure

Thus far, the research presented in this report has concentrated on the circulation features which develop over south Asia in July in two general circulation experiments. In July, the temperatures over south Asia in both experiments have reached a near summer-time maximum and the effects of mountains on the mean July circulation patterns have been clearly identified.

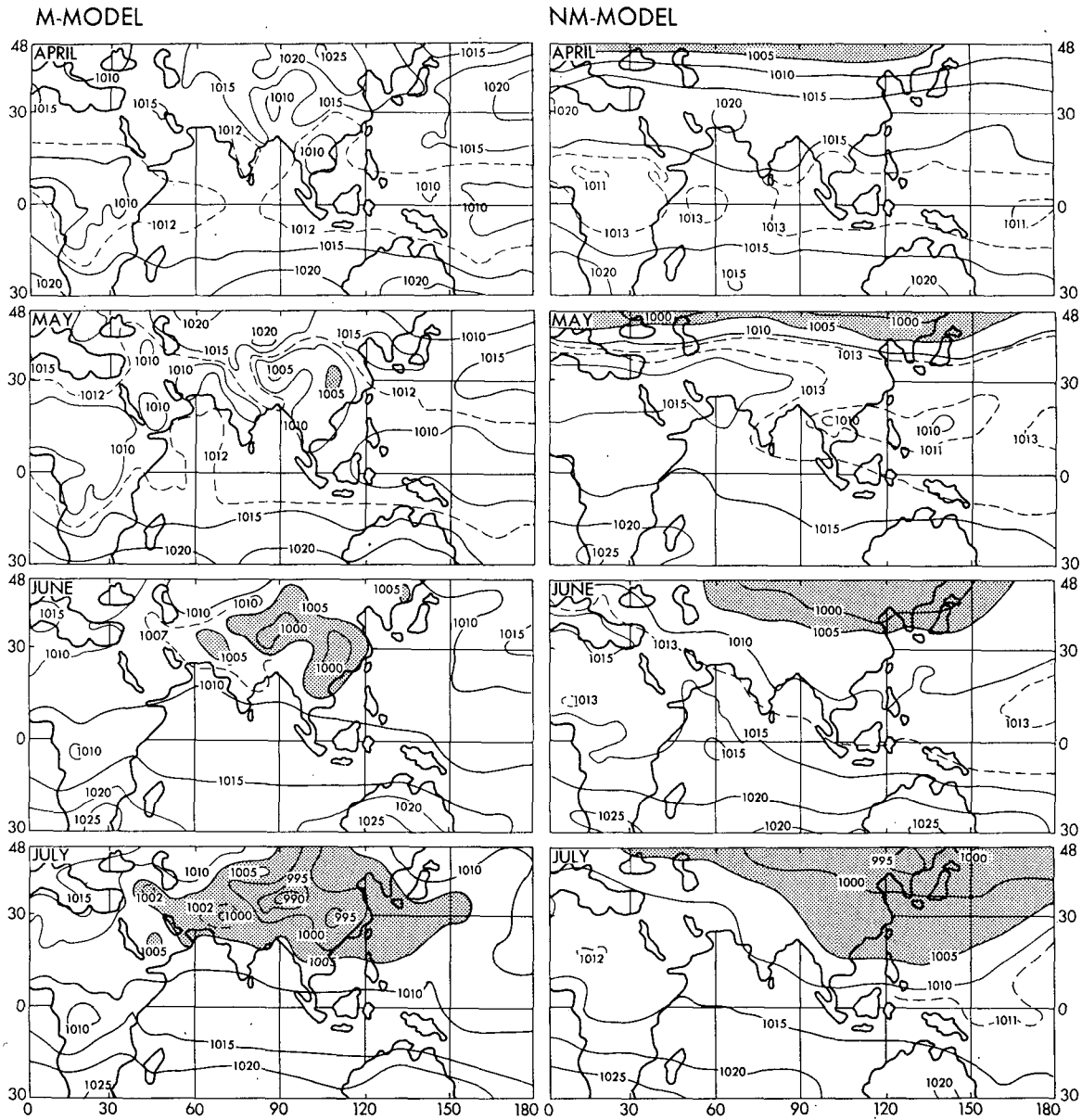

FIG. 5.2. Monthly means of sea level pressure (mb) for the M-model (left) and the NM-model (right).

In this Section, we would like to discuss the effect of mountains on the time-dependent evolution of the monsoon circulation from April through July.

Figs. 5.1 and 5.2 show the monthly mean surface flow and sea level pressure patterns for both the M-model and the NM-model for April through July. In April, the large-scale sea level pressure and surface flow patterns for both models are quite similar, and large-scale features of both models are characterized by high pressure over the continent of Asia and low pressure along the equator. Correspondingly, most of the surface flow between 30°N and the equator has a northerly wind component, and in the Southern Hemisphere southerly flow is directed from the semipermanent subtropical high pressure belt at 30°S toward the equatorial low where the ITCZ can be clearly identified.

In May in the M-model, some of the pressure features of the summer monsoon are beginning to form—low pressure over Tibet and the monsoon trough. However, their intensity is not sufficient to alter the large-scale circulation from that of April. While the continental high still persists at 30°N in May of the NM-model, the equatorial low pressure belt shifts northward over southeast Asia and the western Pacific. Correspond-

ingly, the ITCZ shifts northward to about 8°N at 80°E just south of India.

By June, the effect of mountains on the south Asian monsoon is clearly evident. In June in the M-model, the monsoon trough and large-scale south Asian low pressure belt along 30°N can be easily identified, while in the NM-model, the monsoon trough does not exist and the Asian continental low forms far to the northeast. The surface flow patterns for June reveal that, in the M-model, southerly flow extends northward all the way to the monsoon trough (20°N) and the south Asian low (30°N); this represents an abrupt change from the situation in May when southerly flow was prevalent only in the Southern Hemisphere.

In contrast to the sudden penetration of southerly flow northward to 30°N in June in the M-model (see Section 3), the northward shift of southerly flow in the NM-model is shown to take place at an earlier date, but during May the southerly flow at the surface does not extend far enough northward to reach the Indian peninsula. Over the next two months as the continental air warms, lower pressure replaces the high pressure belt along 30°N, and southerly flow gradually extends northward bringing the monsoon to south India. However, without the assistance of a well-developed low pressure belt over south Asia as found in the M-model, southerly flow is not able to extend northward of 15°N in the NM-model.

In Section 3, the abrupt onset of the monsoon circulation at the surface in the M-model is shown to take place just after the upper tropospheric subtropical jet abruptly shifts northward 20° to a summertime position along 45°N. A latitude-time section (Fig. 5.3), analogous to Fig. 3.7 for the M-model, shows the northward progress of the subtropical jet in the NM-model. Without mountain effects, the subtropical jet does not abruptly jump northward to its summertime position, but rather it slowly moves northward throughout May and June, becoming established in July at a latitude approximately 10° farther south than in the M-model. This figure clearly indicates that in the upper troposphere, as had been previously shown for the surface, the onset of the monsoon circulation is gradual when the mountain effects are neglected.

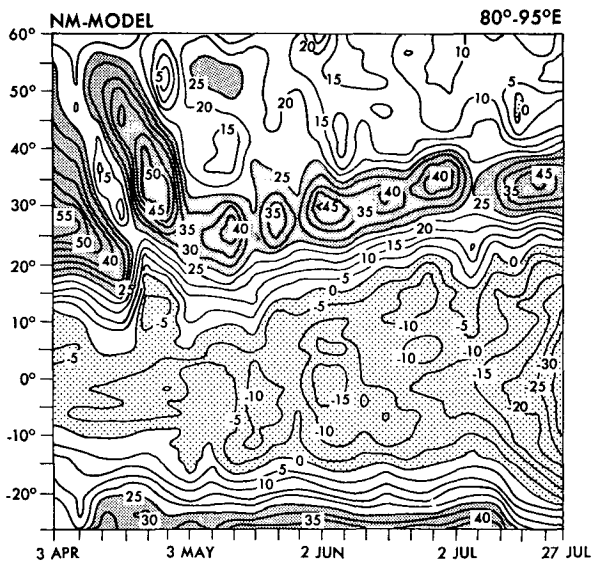

FIG. 5.3. Latitude-time section of zonally averaged (80–95°E) 5-day mean zonal winds (m s^{-1}) at the 190 mb level of the NM-model.

b. Precipitation

Fig. 5.4 shows latitude-time sections of 5-day mean precipitation rate zonally averaged over 80–95°E for both the M- and NM-models. The longitudinal belt corresponds to eastern India, the Bay of Bengal and western Burma, the region just south of the highest portions of the Tibetan Plateau. For the NM-model, this figure reveals the northward shift of the rainbelt around 1–5 May from a latitude at or just south of the equator to a latitude around 8–10°N. The area of maximum rainfall lies approximately along 8–10°N in May, and a gradual northward movement is indicated in June and July. North of the rainbelt in the NM-model, at latitudes corresponding to northern and central India, rainfall is meager as this region was previously shown to be dominated by dry continental northerly flow.

For the M-model, Fig. 5.4 reveals a band of rainfall along 27–30°N which persists even before the onset of the monsoon. This belt of moderately heavy precipitation corresponds to the orographically induced premonsoon rainfall along the southern slope of the Himalayas. The onset of the monsoon rainfall is indicated around 31 May–4 June when the rainbelt abruptly shifts northward to 20°N, slightly south of the monsoon trough. Moderate rainfall persists along the monsoon trough throughout June as the monsoon is most active in June.

In both models between 80 and 95°E, Fig. 5.4 clearly indicates two rainbelts which do not result from mountain effects: along the winter position of the ITCZ at 0–5°S and along its summer position around 10–15°N. In addition, Fig. 5.4 also indicates that there may be important interactions between the preferred latitudes of the rainbelts even after the onset of the monsoon. For the NM-model after the region of maximum rainfall has shifted northward, intense rainfall reappeared at 0–5°S during 5–9 June, and the rainfall associated with the ITCZ at 8–10°N briefly abated. In the M-model, heavy precipitation is found along both rainbelts during late June and late July, and when rainfall decreased in the southern rainbelt during early July, rainfall along the northern rainbelt increased. This indicates that the dynamics which produce rainfall just south of the equator may be important when

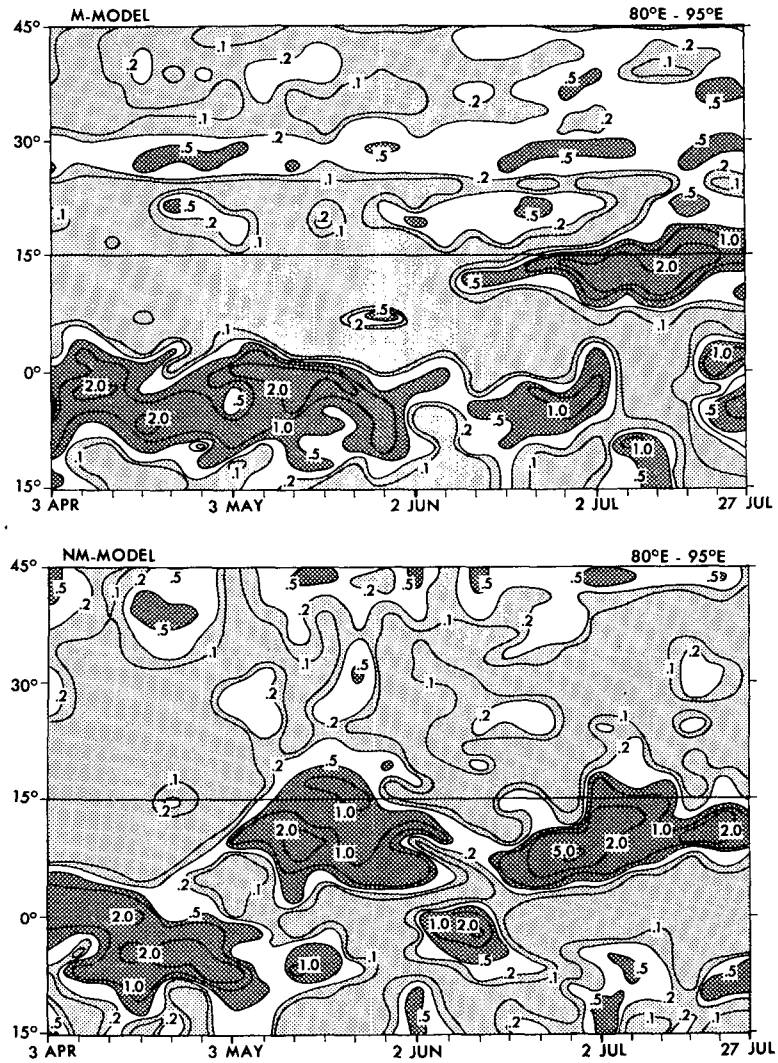

FIG. 5.4. Latitude-time section of 5-day rate of precipitation (cm day^{-1}) averaged from 80–95°E for the M-model (top) and the NM-model (bottom).

describing temporal variations in the monsoon to the north over south Asia.

As previously mentioned, another preferred region of rainfall exists in the M-model just south of the monsoon trough at 20°N. This is not a feature of the NM-model as the monsoon trough owes its existence to the effects of mountains. Fig. 5.4 indicates that there may be important interactions between the monsoon trough and the ITCZ to the south. As time progresses from June into early July in the M-model, rainfall along the monsoon trough decreases and rainfall along the ITCZ south of the monsoon trough becomes more intense. Around 5–9 July rainfall along the monsoon trough is at a minimum, while rainfall along the ITCZ over southern India is at a maximum. Later in July, rainfall again increases along the monsoon trough as it decreases along the ITCZ. A sequence of events similar to the aforementioned is quite often observed over India during the evolution around a period of break monsoon. In contrast, conditions similar to those of break monsoon persist throughout the monsoon season in the NM-model, as rainfall remains heavy along the ITCZ and meager along the monsoon trough.

c. Meridional circulation

In order to explain the monsoon mechanism, Koteswaram and Rao (1963) propose two Hadley circulations and an ITCZ (Fig. 5.5), with the heat source over the monsoon trough and a sink over the cooler oceanic areas to the south. They emphasize that the summer monsoon circulation over India as well as southeast Asia is primarily based on the differential heating between land and sea areas in the Northern Hemisphere. They conclude that the break monsoon reflects the effects of mountains when, in late summer, the increasing temperatures over Tibet produce surface pressures

low enough to attract the monsoon trough (ITCZ) northward to the Himalayan mountain slopes. This explanation for break monsoon does not agree with the observations of Ramamurthy (1969) which suggest that the meridional circulation tends to be reversed over northern and central India during the break monsoon, i.e., the meridional component of the wind near the surface shifts from a southerly to a northerly flow during break monsoon, while in the upper troposphere it tends to shift from northerly to southerly flow during periods of break monsoon.

The NM-model simulation provides a useful tool for determining to what extent the meridional circulation of the monsoon is controlled by the differential heating between land and sea areas. Clearly, the analysis of the NM-model indicates that the south Asian low pressure belt and the smaller scale monsoon trough do not exist if the effects of mountains are not considered. The meridional circulation which develops in the NM-model in response to differential heating of land and sea (Fig. 4.7) is qualitatively similar to that observed by Ramamurthy (1969) for break monsoon and that of Koteswaram and Rao (1963) when their circulation features (Fig. 5.5) are shifted southward approximately 10°.

For a monsoon circulation that results from the combined effects of mountains and land-sea contrast, the numerical experiment results indicate a much more complicated meridional circulation pattern which may vary with time. Fig. 5.4 indicates that, for the M-model, break monsoon conditions prevail during 5-9 July as little precipitation falls at 20°N just south of the monsoon trough. Fig. 5.6 shows 5-day mean meridional circulation profiles before, during and after this period of break monsoon in the M-model. In all three profiles, descending motion is indicated over the monsoon trough. However, during the break monsoon period, the ITCZ and the northern Hadley cell are well-developed with a broad band of strong descending motion extending downward near the surface and southward from the monsoon trough at 20°N into central India. In Fig. 3.5, descending northerly flow is shown to reach down to the surface between 80 and 95°E during this break period. Except for the mountain region, these characteristics of the meridional circulation of the M-model on 5–9 July closely resemble those which persist in the NM-model, as the circulation profiles of both models resemble that described by Ramamurthy (1969) for the break monsoon. Later in July (15–19 July, for example) the northern Hadley cell weakens and southerly flow at the surface becomes stronger north of the ITCZ.

A well-developed northern Hadley circulation over northern and central India accounts for many of the characteristics of the break monsoon. This feature persisting in the NM-model and appearing only briefly in the M-model indicates that the mountain effects are responsible for maintaining an active monsoon rather than a break monsoon as suggested by Koteswaram and Rao (1963).

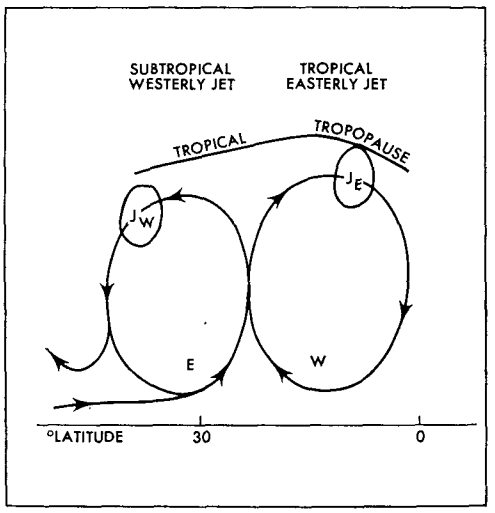

FIG. 5.5. Circulation of the "monsoon cell" from Koteswaram and Rao (1963).

6. Summary and conclusions

The global numerical experiment with mountains is capable of simulating the large-scale July mean sea level pressure and surface flow patterns associated with the south Asian monsoon. Regarding smaller scale pressure patterns and surface circulations, this model simulates the Somali jet, overestimates tropical cyclone activity in the western Pacific, and underestimates the intensity of the monsoon trough and associated monsoon depressions over northern India.

The model with mountains is also capable of simulating the mean July circulation features of the upper troposphere which are associated with the south Asian monsoon. In this model, a large anticyclonic circulation at 190 mb is located over Tibet, which acts as a source region for the easterly jet. Unfortunately, both of these features are located approximately 5° too far south.

The onset of the monsoon is simulated by the M-model. In the upper troposphere, just before the onset of the monsoon at the surface, the westerly jet abruptly shifts from a course around the southern periphery of Tibet to a position approximately 20° latitude farther north. Subsequently, approximately two weeks later than normally observed, the onset of southerly flow near the surface takes place bringing rainfall onto the south Asian subcontinent. Rainfall begins along the southeastern coast of India in the M-model, and over the next month rainfall patterns expand north and westward over India in a way similar to the observed monsoon onset.

The effect of mountains is evidenced when the mean July circulation patterns of the model with mountains

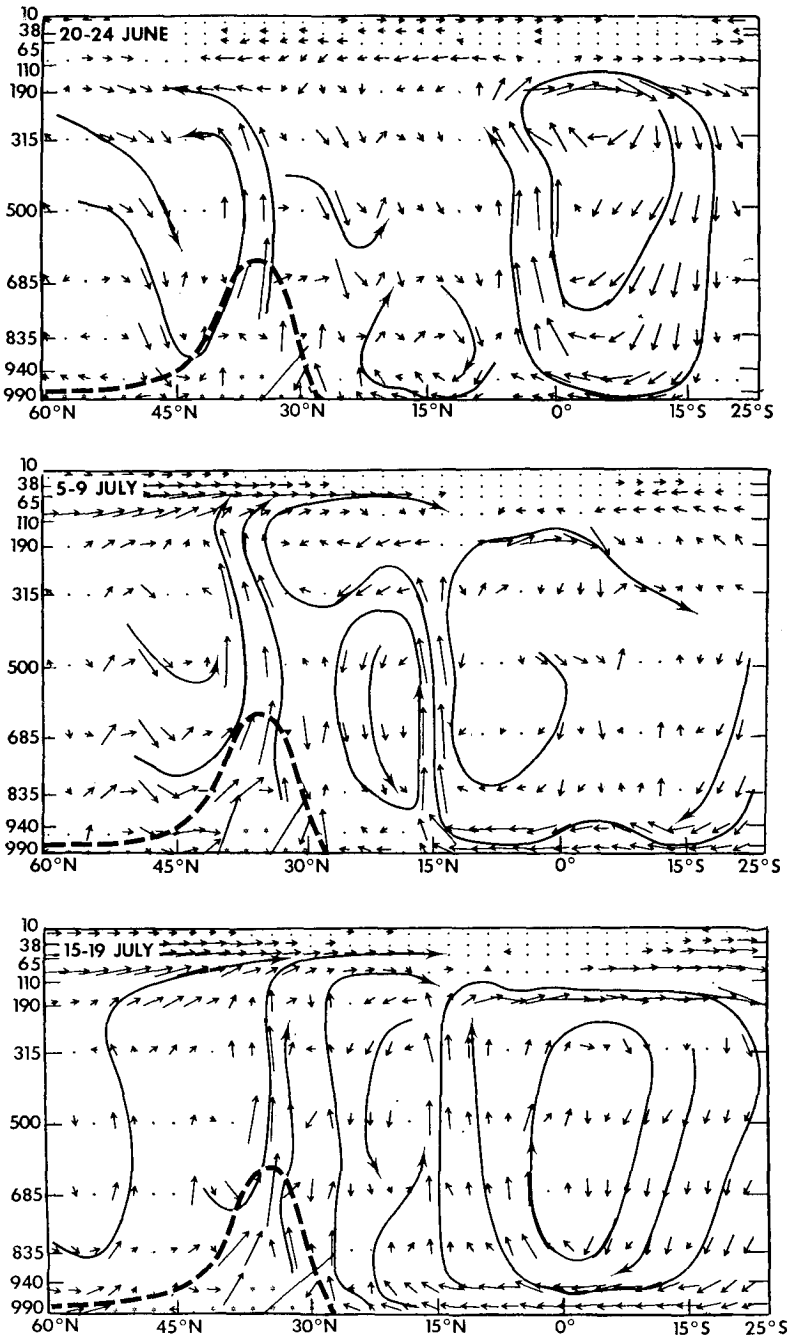

FIG. 5.6. Five-day M-model mean meridional circulation profiles zonally averaged from 55 to 105°E for periods before, during, and after the break monsoon (top to bottom, respectively).

(M-model) are contrasted with those of the model without mountains (NM-model). The effect of the Tibetan Plateau is clear. Over Tibet in July, moist processes and latent heating dominate in the model with mountains; without mountains dry processes (descending motion) and sensible heating dominate over Tibet. Even though surface temperatures are warmer in the NM-model, the middle troposphere is much colder as dry adiabatic lapse rates prevail over and to the south of Tibet. In the model with mountains, because of latent heating due to moist convection, higher temperatures and moist adiabatic lapse rates are more prevalent over Tibet resulting in a low pressure envelope over the mountains—the south Asian low.

Without the effects of mountains, the continental low forms far to the northeast resulting in a weaker south-to-north pressure gradient, particularly over the Arabian Sea.

Existence of the monsoon trough and the northward extension of the outflow from the Somali jet to northern India seems to be dependent on effects of mountains. In both models, an ITCZ forms near 10–15°N. The Hadley cell north of the ITCZ is usually much weaker when effects of mountains are included. North of the ITCZ in the NM-model, a dry northwesterly flow, rather than the moist southwesterly flow of the M-model, prevails at the surface over most of south Asia. As a result in the NM-model north of the ITCZ, rainfall is persistently meager, resembling break monsoon conditions, whereas in the M-model rainfall tends to be more moderate. Clearly, without mountains, a more continental climate extends southward over south Asia rather than the monsoon climate extending farther northward into Asia.

Mountains also have an important effect on the onset and temporal variations of the south Asian monsoon. At the time of onset, humid southerly flow suddenly extends northward from the equator to the monsoon trough (20°N) and the south Asian low (30°N) in the model with mountains; in the model without mountains humid southerly flow extends northward to about 8–12°N initially, and then over the next two months it continues to slowly migrate northward to about 15°N, never reaching northward to central India or Tibet. In the upper troposphere of the model without mountains, the subtropical jet slowly moves northward from 25 to 35°N over a period of about two months; this is in sharp contrast to the behavior of the subtropical jet in the model with mountains where it is shown to abruptly jump northward from 25 to 45°N over a period of only a few days.

Three preferred latitudes of upward motion exist in the M-model: over the wintertime position of the ITCZ near the equator, along the ITCZ which develops in July near 15°N, and along the monsoon trough and south Asian low pressure system. Without mountains only the first two exist, as the monsoon trough and the south Asian low owe their existence to the effect of mountains. Significant interplay is indicated between these preferred regions of upward motion in both models, and often when upward motion in one preferred region is intense producing copious precipitation, rainfall at another preferred region of upward motion abates.

After these experiments, it is unclear why the monsoon trough in the M-model is systematically weaker than observed. Clearly, mountain effects contribute to lowering pressure over south Asia and the monsoon trough. Manabe and Holloway (1975) noted that the ability of the present model in simulating climate deteriorates in the neighborhood of steep mountains. Further improvement of the formulation as well as the resolution of finite differencing may be essential for eliminating this problem. These experiments also suggest further observational research regarding the position and intensity of the ITCZ as the monsoon cycles through various stages of active monsoon and break monsoon. The role of the area of mean convergence near the equator should also be studied, particularly as to how it interacts with the south Asian monsoon to the north.

Acknowledgments. The authors are indebted to Dr. J. Smagorinsky for his support and encouragement of this study. It is a pleasure to acknowledge J. L. Holloway, Jr., who was mainly responsible for programming the general circulation model used in this study. Special acknowledgment also goes to J. Shukla who gave us many useful comments on the results of the numerical experiments. We wish to express our appreciation to D. Daniel for his programming assistance which was instrumental for the smooth running of the model integrations, and to L. Dimmick for creating many of the visual displays. We thank Drs. Y. Hayashi, A. Oort, and H. Flohn who reviewed the manuscript. Assistance provided by E. Green, P. Tunison, M. Callan, E. Groch, H. Kaufman, J. Conner, and E. Thompson was indispensible in the preparation of the figures and manuscript.

APPENDIX

Sea Surface Temperatures

Sea surface temperatures are imposed at the lower boundary of these seasonal march experiments by interpolating daily in time among four observed monthly mean sea surface temperature distributions (February, May, August, November) taken from the revised data of the U. S. Hydrographic Office (1964). The time interpolation is accomplished by applying a simple Fourier analysis of the form

$$T(t)=\bar{T}+A_1 \sin at+B_1 \cos at+B_2 \cos 2at$$

once each day at each model grid point at time t. For polar regions, $T(t)$ is restricted so that if the calculated value falls below freezing, $T(t)$ is then set to the observed temperature at that location for the coldest of the four months. Consequently, monthly mean sea surface temperatures imposed as a lower boundary condition may differ from those of the observed data source, particularly for intermediate months. Horizontal distributions of monthly mean sea surface temperatures for the south Asian region as calculated using the above scheme are shown in Fig. A1.

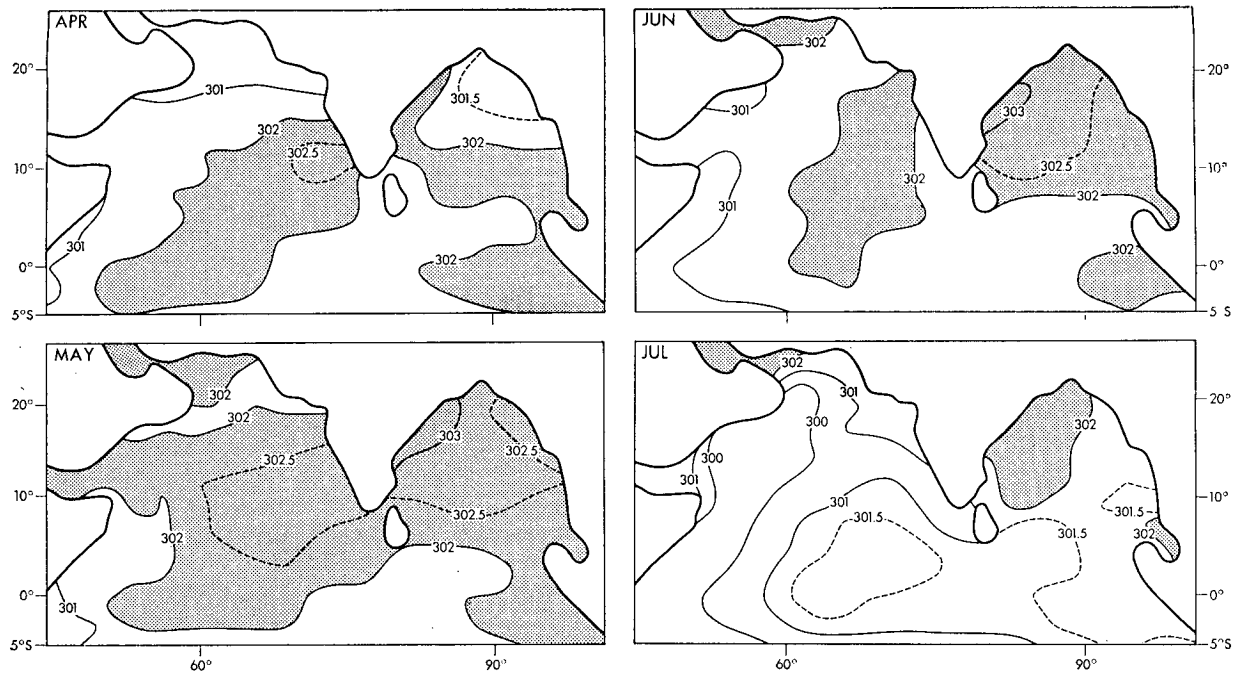

FIG. A1. Horizontal distributions of monthly means of imposed sea surface temperatures (K) for both models.

REFERENCES

Ananthakrishnan, R., and K. L. Bhatia, 1958: Tracks of monsoon depressions and their recurvature towards Kashmir. *Proc. Symp. Monsoons of the World*, New Delhi, Hind Union Press, 157–172.

——, and P. J. Rajagopalachari, 1964: Pattern of monsoon rainfall distribution over India and neighbourhood. *Proc. Symp. Tropical Meteorology*, Rotorua, New Zealand, November 1963, New Zealand Meteor. Service, Wellingon [Available at NOAA Atmospheric Sciences Library, Silver Spring, Md. 20910, No. MI5.5S89pr.]

Banerji, Sudhansu Kumar, 1929: The effect of the Indian mountain ranges on the configuration of the isobars. *Indian J. Phys.*, **4**, 477–502.

——, 1930: The effect of the Indian mountain ranges on air motion. *Indian J. Phys.*, **5**, 699–745.

Findlater, J., 1969: Interhemispheric transport of air in the lower troposphere over the western Indian Ocean. *Quart. J. Roy. Meteor. Soc.*, **95**, 400–403.

Flohn, H., 1950: Studien zur allgemeinen Zirkulation der Atmosphäre III. *Ber. Deut. Wetterd.*, **18**, 34–50.

——, 1953: Wilhelm Meinardus und die Revision unserer Vorstellung von der atmosphärischen Zirkulation. *Z. Meteor.*, **7**, 97–108.

——, 1960: Recent investigations on the mechanism of the "Summer Monsoon" of Southern and Eastern Asia. *Proc. Symp. Monsoons of the World*, New Delhi, Hind Union Press, 75–88.

——, 1968: Contributions to a meteorology of the Tibetan Highlands. Atmos. Sci. Paper No. 130, Colorado State University, 120 pp. [Available from National Technical Information Service, Springfield, Va. 22161, No. PB-182 255.]

Halley, E., 1686: An historical account of the trade winds and monsoons observable in the seas between and near the tropics with an attempt to assign the physical cause of the said winds. *Phil. Trans. Roy. Soc. London*, **16**, 153–168.

Hayashi, Y., 1974: Spectral analysis of tropical disturbances appearing in a GFDL general circulation model. *J. Atmos. Sci.*, **31**, 180–218.

Holloway, J. L., Jr., and S. Manabe, 1971: Simulation of climatology by a global general circulation model. *Mon. Wea. Rev.*, **99**, 335–370.

Hydrographic Office, U. S. Navy, 1964: *World Atlas of Sea Surface Temperature*. 2nd ed. H. O. Publ. No. 225, with supplements. [Available from Defense Mapping Agency Depot, 5801 Tabor Ave., Philadelphia, Pa. 19120.]

Koteswaram, P., and N. S. B. Rao, 1963: The structure of the Asian summer monsoon. *Aust. Meteor. Mag.*, **42**, 35–56.

Krishnamurti, T. N., S. M. Daggupaty, J. Fein, M. Kanamitsu and J. D. Lee, 1973: Tibetan high and upper tropospheric tropical circulations during northern summer. *Bull. Amer. Meteor. Soc.*, **54**, 1234–1249.

Kurihara, Y., and J. L. Holloway, Jr., 1967: Numerical integration of a nine-level global primitive equations model formulated by the box method. *Mon. Wea. Rev.*, **95**, 509–530.

Manabe, S., D. G. Hahn and J. L. Holloway, Jr., 1974: The seasonal variation of the tropical circulation as simulated by a global model of the atmosphere. *J. Atmos. Sci.*, **31**, 43–83.

——, and J. L. Holloway, Jr., 1975: The seasonal variation of the hydrologic cycle as simulated by a global model of the atmosphere. *J. Geophys. Res.*, **80**, 1617–1649.

——, and T. B. Terpstra, 1974: The effects of mountains on the general circulation of the atmosphere as identified by numerical experiments. *J. Atmos. Sci.*, **31**, 3–42.

Miller, D., 1971: *Global Atlas of Relative Cloud Cover 1967–1970 Based on Data from Meteorological Satellites*. U.S. Department of Commerce/NOAA/NESS and U. S. Air Force/Air Weather Service, Washington, D. C., p. 66. [Available from National Technical Information Service, Springfield, Va. 22161, No. AD-739 434.]

Mintz, Y., 1965: Very long term global integration of the primitive equation of atmospheric motion. WMO Tech. Note 66,

Proc. WMO-IUGG Symp. Research and Development Aspects of Longe Range Forecasting, 141–161.

——, and G. Dean, 1952: The observed mean field of motion of the atmosphere. *Geophys. Res. Papers*, No. 17, 65 pp.

Möller, F., 1951: Viertel Jahrs karten des Niederschlags für die Ganze Erde. *Petermanns Geograph. Mitt.*, **95**, 1–7.

Murakami, T., R. V. Godbole and R. R. Kelkar, 1970: Numerical simulation of the monsoon along 80E. *Proc. Conf. Summer Monsoon Southeast Asia*, C. S. Ramage, Ed., Norfolk, Va., Navy Weather Res. Facility, 39–51. [Available from National Technical Information Service, Springfield, Va. 22161, No. AD-876-677.]

Newell, R. E., J. W. Kidson, D. G. Vincent and G. J. Boer, 1972: *The General Circulation of the Tropical Atmosphere and Interactions with Extratropical Latitudes*. The MIT Press, 258 pp.

Orgill, M. M., 1967: Some aspects on the onset of the summer monsoon over Southeast Asia, Dept. Atmos. Sci., Colorado State University, Final Report, Contract DA28-043-AMC-0130 3(E), 75 pp. [Available from National Technical Information Service, Springfield, Va. 22161, No. AD-819 959.]

Phillips, N. A., 1957: A co-ordinate system having some special advantage for numerical forecasting. *J. Meteor.*, **14**, 184–185.

Ramage, C., 1971: *Monsoon Meteorology*. Academic Press, 296 pp.

——, R. F. Miller and C. Jefferies, 1972: *Meteorological Atlas of the International Indian Ocean Expedition*, Vol. 1. National Science Foundation, Washington, D. C. [Superintendent of Documents, Washington, D. C., Stock No. 3800-00123.]

——, and C. V. R. Raman, 1972: *Meteorological Atlas of the International Indian Ocean Expedition*, Vol. 2. National Science Foundation, Washington, D. C. [Superintendent of Documents, Washington, D. C., Stock No. 3800-00124.]

Ramamurthy, K., 1969: Monsoons of India: Some aspects of the "break" in the Indian southwest monsoon during July and August. *India Meteorological Department Forecasting Manual*, Part IV, No. N–18, 3. [Available from Director General of Observatory, India Meteorological Department, Lodi Rd., New Delhi 3, India.]

Rangarajan, S., 1963: Thermal effects of the Tibetan Plateau during the Asian monsoon season. *Aust. Meteor. Mag.*, **42**, 24–34.

Riehl, Herbert, 1959: On production of kinetic energy from condensation heating. *The Atmosphere and the Sea in Motion*, The Rossby Memorial Volume, New York, The Rockefeller Institute Press, 381–399.

Sadler, J. C., 1972: Mean upper tropospheric circulation of the tropics. Dept. of Meteorology, University of Hawaii, NSF Grant GS36301. [Available from J. C. Sadler, Dept. of Meteorology, University of Hawaii, Honolulu 96822.]

Shukla, J., 1975: Effect of Arabian sea-surface temperature anomaly on Indian summer monsoon: A numerical experiment with the GFDL model. *J. Atmos. Sci.*, **32**, 503–511.

Smith, S. M., H. W. Menard and G. F. Sharman, 1966: Worldwide ocean depths and continental elevations averaged for areas approximating one degree squares of latitude and longitude. S.I.O. Reference Report 65-8, Scripps Institution of Oceanography, La Jolla, 14 pp. [Available from National Technical Information Service, Springfield, Va., 22161, No. AD-632-530.]

Staff Members Academia Sinica, Inst. Geophys. Meteor. Peking, 1957–58: On the general circulation over Eastern Asia I–III. *Tellus*, **9**, 432–446; *Tellus*, **10**, 58–75 and 299–312.

Walker, J. M. 1972: The monsoon of southern Asia: A review. *Weather*, **27**, 178–189.

Washington, W. M., and S. M. Daggupaty, 1975: Numerical simulation with the NCAR global circulation model of the mean conditions during the Asian-African summer monsoon. *Mon. Wea. Rev.*, **103**, 105–114.

Yeh, Tu-Cheng, Dao Shih-Yen and Li Mei-Ts'un, 1959: The abrupt change of circulation over the Northern Hemisphere during June and October. *The Atmosphere and the Sea in Motion*, Rossby Memorial Volume, New York, The Rockefeller Institute Press, 249–267.

Yin, Maung Tun, 1949: A synoptic-aerologic study of the onset of the summer monsoon over India and Burma. *J. Meteor.*, **6**, 393–400.